*Journal of Theoretics*

Journal Home Page

# Application of BSM Atomic Models for Theoretical Analysis of Biomolecules

S. Sarg
sarg@helical-structures.org

**Abstract:** The proteins have amazing properties of guiding the energy along their long chains and preserving own three-dimensional structure in proper environments. These features cannot obtain satisfactory explanations by the quantum mechanical models of the atoms. A wide range interdisciplinary study, using a different theoretical approach, indicates that the quantum mechanical models do not describe the full physical features of the real atoms. Based on an alternative concept about the physical vacuum, a recently developed Basic Structures of Matter (BSM) theory allows unveiling the physical structures of the elementary particles and their spatial arrangement in the atomic nuclei. The obtained physical models of the atoms exhibit the same energy levels as the quantum mechanical models, while the positions of the electron orbits are defined by the nuclear structure. The derived atomic models allow studying the physical conditions behind the structural and bond restrictions of the atoms connected in molecules. The existing data base about the atomic structural compositions of the organic and biomolecules provides an excellent opportunity for test and validation of the derived physical models of the atoms. The presented article demonstrates a new original method for theoretical analysis of biomolecules. The analysis of DNA molecule, leads to a formulation of hypotheses about an energy storage mechanism in proteins and a possible involvement of DNA in cell cycle synchronization. The analysis of tRNA molecule leads to formulation of hypothesis about a binary decoding mechanism behind the 20 flavors of the complex of the aminoacyle-tRNA synthetases with tRNA.

**Keywords:** Structure of biomolecules, secondary structure of proteins, molecular structure of DNA, Levinthal's paradox, C-value paradox, twenty flavors, aminoacyl-tRNA synthetases.

# Application of BSM atomic models for theoretical analysis of biomolecules. Hypotheses: 1. Energy storage mechanism in biomolecules; 2. DNA involvement in cell cycle synchronization; 3. Binary decoding mechanism behind the twenty flavors in aminoacyl-tRNA synthetases.

S. Sarg
sarg@helical-structures.org

**Abstract** The proteins have amazing properties of guiding the energy along their long chains and preserving own three-dimensional structure in proper environments. These features cannot obtain satisfactory explanations by the quantum mechanical models of the atoms. A wide range interdisciplinary study, using a different theoretical approach, indicates that the quantum mechanical models do not describe the full physical features of the real atoms. Based on an alternative concept about the physical vacuum, a recently developed Basic Structures of Matter (BSM) theory allows unveiling the physical structures of the elementary particles and their spatial arrangement in the atomic nuclei. The obtained physical models of the atoms exhibit the same energy levels as the quantum mechanical models, while the positions of the electron orbits are defined by the nuclear structure. The derived atomic models allow studying the physical conditions behind the structural and bond restrictions of the atoms connected in molecules. The existing data base about the atomic structural compositions of the organic and biomolecules provides an excellent opportunity for test and validation of the derived physical models of the atoms. The presented article demonstrates a new original method for theoretical analysis of biomolecules. The analysis of DNA molecule, leads to a formulation of hypotheses about an energy storage mechanism in proteins and a possible involvement of DNA in cell cycle synchronization. The analysis of tRNA molecule leads to formulation of hypothesis about a binary decoding mechanism behind the 20 flavors of the complex of the aminoacyle-tRNA synthetases with tRNA.

**Keywords***: Structure of biomolecules, secondary structure of proteins, molecular structure of DNA, Levinthal's paradox, C-value paradox, twenty flavors, aminoacyl-tRNA synthetases.*

## 1. Introduction

*Note*: *The numbering of the equations and figures given in square brackets corresponds to their numbering in the monograph*[1] *where a detailed analysis and derivation is provided.*

Despite the huge number of possible configurations of the atoms in the proteins, according to the Quantum mechanics, they fold reliably and quickly to their native state. From a point of view of the Quantum mechanical considerations, this effect, known as a Levinthal's paradox, is not explainable. According to them, a protein molecule of 2,000 atoms, for example, should possess an astronomical number of degrees of freedom. The observations show that this number is drastically reduced by some strong structural restrictions, such as bond lengths, and restricted angle range of bond connections and rotations. The stable appearance of the secondary and tertiary structures of the proteins indicates also that some additional restrictions take place in a proper environment. All this restrictions could not get satisfactory explanation by the Quantum mechanical models of the atoms. While these models rely heavily on the the uncertainty principle, the quite deterministic structure and behaviour of the complex molecules like proteins do not show its signature.

An extensive interdisciplinary study[1] from different fields of physics indicates that the Quantum mechanical models of the atoms are rather mathematical models than physical ones, so they are not able to provide all the features that the real atoms possess. The same study also shows that the atomic models are strongly dependable of the concept of the physical vacuum. This concept has been

changed four times in the history of the physics[2,3] . The adopted by the contemporary physics concept still could not be considered as a final truth. The results of the study led to development of an original unified field theory called Basic Structures of Matter (BSM)[1]. In order to build such theory, however, the concept of the vacuum had to be reconsidered once again. The developed BSM theory from its hand allowed derivation of quite different physical models of the atoms, possessing rich physical structures, while characterized by the same energy level of excitation. The unveiled structural features of the atoms are not apparent from the quantum mechanical atomic models, operating only by energy levels, while assuming that the physical vacuum is an empty space, not possessing a matter.

The purpose of the initial part of this article (sections 2 to 9) is to acquaint very briefly the scientist from the field of molecular biology with the concept of the BSM theory and particularly with the derived physical models of the atoms.

The second part of the article (sections 10 to 11) shows the potential application of the BSM concept and the derived atomic models for studying the properties of the biomolecules. The theoretical analysis of some features of DNA and tRNA leads to formulation of three hypotheses.

While the BSM concept is quite original, the reader who want becoming familiar in details with its arguments outputs should be acquainted with the article[4] "Brief introduction to BSM theory and derived atomic models" (Journal of Theoretics, online access)) or with the theory[1].

## 2. The new point of view of the BSM theory

Extensive analysis of phenomena from different fields of physics, indicates that the vacuum is not a void space, but possessing a underlying grid structure of sub-elementary particles arranged in nodes. These particles called twisted prisms are formed of two types super dens intrinsic matter substances. Prisms of the same type are attracted in a pure void space by Intrinsic Gravitational (IG) forces, $F_{IG}$, that are inverse proportional to a cube of the distance.

$$F_{IG} = G_0 \frac{m_{o1} m_{o2}}{r^3} \qquad [(2.1)]$$

where: $m_{o1}$ and $m_{o2}$ are intrinsic masses (of this superdense particles), $G_o$ is the Intrinsic Gravitational constant valid for pure void space.

It is assumed that the IG force is related to the well known physical parameter called Planck's frequency, $\omega_{PL}$

$$\omega_{PL} = \sqrt{\frac{2\pi c^5}{G}} \qquad (1)$$

This assumption is in agreement with the theoretical work of H. E. Puthoff[5] (1989) showing a derivation of the Newton's law of gravitation, based on the Plank's frequency and using one hypothesis of Sakharov.

According to BSM concept, every node of the underlying vacuum grid is comprised of four prisms of same substance held by IG forces, so its geometry is flexible. The prisms possess axial IG anisotropy with a twisting component, due to a lower level structure, so they are called twisted prisms. The Intrinsic Gravitation (IG) appears as a type of energy interaction between intrinsic matter at lower level of matter organization involved in an intrinsic energy balance. The gaps between the alternatively arranged nodes of different types are also kept by an intrinsic energy balance. The estimated distance between neighbouring nodes of the grid is in order of (1 ~ 2)E-20 (m), while the matter density of the prisms is about 1E13 times higher than the density of the average atomic matter. It is called a Cosmic Lattice (CL), so the physical vacuum in BSM theory is referenced as a CL space.

The self-sustainable CL structure is supported by super strong interactions between the highly dens intrinsic matter from which the prisms are built. The elementary particles are build by the same prisms and comprised of spatially ordered helical shells called helical structures possessing also internal lattice formed from the same prisms. The only forces responsible for holding the twisted prisms in both: the CL structure and the structure of the elementary particles are the IG forces. The CL structure of the physical vacuum penetrates not only in all aggregate states of the atomic matter but partly in the elementary particles as well. The Newtonian mass (the mass we are familiar with) is expressible as a CL static pressure exercised on the internal volume structure of the particle that is not penetrative to the CL node structure. The Newto-

nian gravitation is a propagation of the IG field through the CL space in a distance much longer than the CL node distance (by the self aligned prisms of the neighbouring CL nodes). At close distances between particles, atoms and molecules, however, the IG forces leak through CL space causing an attraction stronger than the Newton's gravity (Casimir forces and some of Van der Wall's forces. Such effect is explainable when taking into account that the matter density in the prisms is about 1E13 times higher than the average atomic matter.

A massive object such as a star, a planet or a moon, has an ability to hold the CL space structure up to some extend, defining in such way the conditions of General relativity. CL space has specific features of possessing distributed Zero Point Energy and conditions for gravitational, electrical and magnetic field. Another specific features of the CL space is the ability of the CL nodes to fold and pass through the grid structure of a normal CL space when a less massive object moves in a CL space of a more massive one. This feature is behind the inertial properties of the atomic matter in CL space and the equivalence between gravitational and inertial mass. The prisms are formed in an unique formation process existing in a hidden phase of a galaxy evolution govern by IG forces and fundamental matter-energy process.

Fig. 2.20 illustrates a geometry of a single node in position of geometrical equilibrium with two sets of axes, denoted as *abcd* and *xyz*.

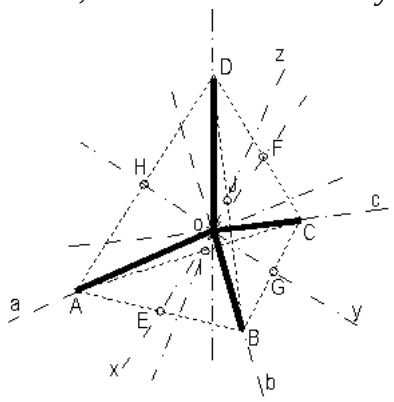


Fig. 2.20 CL node in geometrical equilibrium position
The two sets of axes are: *abcd* and *xyz*

The CL node has two sets of axes: one set of 4 axes along anyone of the prisms called *abcd* axes, and another set of 3 orthogonal axes called *xyz* axes. In geometrical equilibrium the angles between anyone of abcd axes is 109.5$^{o}$. The *abcd* axes define a tetrahedron. The *xyz* axes pass through the middle of every two opposite edges of the tetrahedron. In the same time, the orthogonal *xyz* axes of the neighbouring CL nodes are aligned. Such arrangement gives conditions for complex node oscillations under the inverse cubic law of Intrinsic Gravitation. The return forces (of inverse cubic law) acting on deviated from the central position CL node exhibits set of minimums. These minimums can be associated with energy wells. **Two symmetrical minimums appear along anyone of *xyz* axes and one minimum along the positive direction of anyone of *abcd* axes.** These set of minimums provide conditions for complex oscillations of the CL node. From a dynamical aspect these minimums contribute to the total energy well of the CL node (Zero Point Energy of vacuum). Fig. [2.24] illustrates the return forces along the two sets of axes and the associated with them energy wells. The right vertical axis indicates specific energy points. The energy level $E_{C2}$ corresponds to the filled energy wells or the Zero Point Energy of the vacuum.

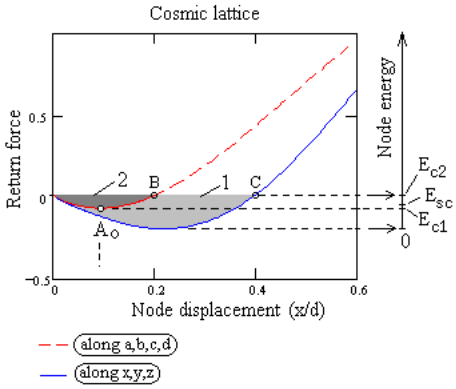


**Fig. [2.24]**

The complex oscillation of the CL node is well described by two vectors: a Node Resonance Momentum (NRM) and a Spatial Precession Momentum (SPM). The NRM vector is related to the light velocity expressed by one resonance cycle of CL node per node distance. The SPM vector is related to the permeability and permittivity of the vacuum. The frequency of the SPM vector is the well known Compton frequency. Analysing the dynamics and mutual interactions of the CL nodes (§2.9 of BSM theory), it is possible to understand some of the fundamental physical parameters, such

as: unite charge, magnetic field, Planck constant, Zero Point Energy, photon wavetrain structure, light velocity, permeability and permittivity of vacuum.

From a BSM point of view, the interpretation of the scattering experiments does not provide correct real dimensions of the elementary particles, because their structures and the CL space structure of the vacuum are not taken into account. BSM analysis found that the stable particles, such as proton, neutron and electron (and positron) posses structures with well defined spatial geometry and denser internal lattices. They are comprised of complex but understandable three-dimensional helical structures whose elementary building blocks are the same as those involved in the vacuum grid - the two types of prisms. Analysing the interactions between the vacuum space and elementary particles, but from a new point of view, the BSM theory allowed a derivation of number of useful equations, such as a light velocity equation - expressed by the CL space parameters, a mass equation (the mass we are familiar with), an equation about the vacuum energy (zero point energy), and some relations between CL space parameters and the known physical constants. The BSM provides also an understandable physical explanation of what is an elementary electrical charge and why it is constant.

The motion analysis of the smallest charge particle - the electron from a new point of view (Chapter 3 and 4 of BSM) allows to unveil its physical structure and intrinsic properties. The electron is a system comprised of three helical structures as illustrated by Fig. 2. Two of its helical structures possess denser lattices located in the internal space of the helix envelopes (not shown in Fig. 2).

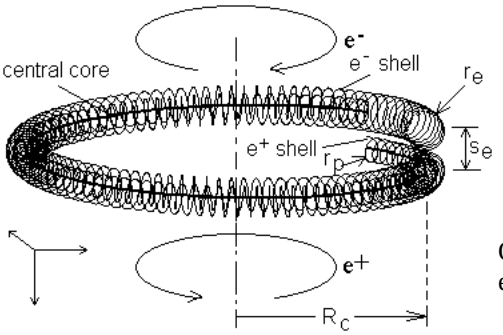


Fig. 2
Oscillating electron

The physical dimensions of this structures are: $R_C$ - Compton radius of electron (known), $r_e$ - a small electron radius, $r_p$ a small positron radius, $s_e$ - helix step.

External helical structure with internal denser lattice (from right handed prisms, for example) is referenced in BSM as external electron shell. It is responsible for the modulation of the CL space around the electron that we detect as an electrical charge. The internal helical structure with internal denser lattice (from a left-handed prisms, respectively) with a central core (from right handed prisms) is an internal positron. Regarded as a 3 body oscillating system, the electron has two proper frequencies:

- a first proper frequency: between the external electron shell and the internal positron
- a second proper frequency: between the internal positive shell and the central negative core.

It is found that the first proper frequency of the electron is equal to the frequency of the SPM vector of the oscillating CL node. The frequency of the SPM vector appears to be the well known Compton frequency.

It conditions of screw-like motion of the electron with tangential velocity equal to the light velocity, the phase of the first proper frequency of the rotating electron matches the phase of the SPM vector of CL nodes. They both oscillate with a Compton frequency. In the same time, the internal core oscillation (with a proper frequency of three times the Compton frequency) provides a third harmonic feature for this motion. As a result the rotating and oscillating electron exhibit a maximum interaction with the CL space - a kind of quantum interaction. The electron axial velocity for this case is $v_{ax} = \alpha c$, corresponding to kinetic energy of 13.6 eV. In such type of motion the helical step of the electron, $s_e$, is estimated by the following relations:

$$s_e = \frac{2\pi R_c \alpha}{\sqrt{1-\alpha^2}} = \frac{\lambda_c \alpha}{\sqrt{1-\alpha^2}} = 1.7706\times10^{-14}\ \text{(m)} \qquad [(3.9)]$$

$$s_e = g_e r_e = 2.002319 r_e \qquad [(3.12.a)]$$

where: $R_c$ - is the Compton radius, $\alpha$ - is the fine structure constant, $g_e$ - is the gyromagnetic factor, $\lambda_c$ - is the Compton wavelength (CL space parameter).

From the analysis of the Fractional Quantum Hall experiments in Chapter 4 of BSM, it is found that: $r_p/r_e = 2/3$. Then all the of geometrical parameters of the electron are determined.

The confined screw like motion of the oscillating electron in CL space is characterized by strong quantum interactions with the oscillating CL nodes. This effect is contributed by two conditions: a phase match between the involved cycles (discussed above) and conditions of integer number of Compton wavelengths for boundary conditions of the induced magnetic field from the rotating electron[4] (more details in Chapter 3 of BSM). These two conditions allow strong quantum effects to appear at particular velocities of screw-like motion of the electron, corresponding to the energy levels of 13.6 eV, 3.4 eV, 1.51 eV, 0.85 eV and so on.

**The magnetic radius $r_{mb}$ in a plane normal to $V_{ax}$ is defined from the conditions that the rotating IG field of the internal lattice of the electron helical structure (that modulates the CL space) could not exceed the light velocity.**

The magnetic radius for 13.6 eV is verified from the analysis of the quantum magnetic field (see §3.11 in Chapter 3 of BSM thesis): $\Phi_0 = h/q_o$ The accurate value of $r_{mb}$ for 13.6 eV is almost equal to $R_C$, but slightly larger due to a finite thickness of the electron helical structure.

If relating the above energy levels with the number of full rotations of the electron one obtains:

13. 6 eV - 1 rotation per SPM cycle
3.4 eV - 1/2 rotations per SPM cycle
1.51 eV - 1/3 rotations per SPM cycle
0.85 eV = 1/4 rotations per SPM cycle
1 SPM cycle = Compton time

BSM uses a parameter called **subharmonic number**, *n*, in order to notify the quantum motion conditions of the electron. This number is related to the electron axial velocity by the expression $V_{ax} = \alpha c/n$. In the same time the subharmonic number matches the quantum number of the electron orbit in Bohr atomic model. A quantum motion with a first harmonic velocity corresponds to 13.6 eV; a motion with a second subharmonics - 3.4 eV; a motion with a third subharmonics - 1.51 eV and so on. The term subharmonic number is chosen because it annotates the spin rotation of the electron in its confined motion. The strength of the quantum interaction with the CL space decrease with increasing of *n*.

Analysing the efficiency of the quantum interactions between the confined moving electron and CL space at relativistic velocities the relativistic gamma factor is derived in §3.11.A. (BSM Chapter 3). The analysis provides a physical explanation of the relativistic effect of mass increase. It is a result of the finite rate at which the CL node could be folded and displaced. A limiting factor of this rate is the resonance frequency of CL node, estimated in §2.11.3, Chapter 2 of BSM, as:

$$\nu_R = 1.092646\times10^{29} \text{ (Hz)} \qquad [(2.55)]$$

## 3. Quantum loops and possible orbits for electron with optimal confined velocity. Embedded signature of the fine structure constant.

### 3.1 Quantum motion of the electron in closed loop trajectories.

The motion of the electron is always a result of external forces. The orbital motion of the electron could be regarded as motion in closed loop, whose trajectory follows equipotential surface of electrical field defined by one or more positive charges. All this conditions are ideal for a quantum motion of the electron in a closed loop.

The analysis of the confined motion of the oscillating electron in closed loop[4], leads to the conclusion:

**(A) The number of cycles of the first and second proper frequency of the electron in the orbital trace is defined only by the fine structure constant.**

In the same article[4] it is shown that the conditions of accurate phase match between the first and second proper frequency of the electron in its confined quantum motion in a closed loop is satisfied for **2573380** full turns of the electron in which the the expression is valid

$$1/\alpha^3 = integer = 2573380$$

The CODATA 98 $\alpha = 7.2973525(27)\times10^{-3}$ is the closest value of the fine structure constant satisfying the above expression.

The introduced by BSM theory subharmonic number (n) of the moving and oscillation electron corresponds to the principal quantum number of Bohr model.

*Table 1* shows the quantum motion parameters of the electron in a quantum loop for different number *n*.

**Table 1**

| No | $E$ (eV) | $V_{ax}$ | $V_t$ | $r_{mb}$ | $l_{ql}$ | $L_q$ (A) |
|---|---|---|---|---|---|---|
| 1 | 13.6 | $\alpha c$ | $c$ | $\sim R_c$ | $2\pi a_0$ | 1.3626 |
| 2 | 3.4 | $\alpha c/2$ | $c/2$ | $2R_c$ | $2\pi a_0/2$ | 0.6813 |
| 3 | 1.51 | $\alpha c/3$ | $c/3$ | $3R_c$ | $2\pi a_0/3$ | 0.4542 |
| 4 | 0.85 | $\alpha c/4$ | $c/4$ | $4R_c$ | $2\pi a_0/4$ | 0.3406 |
| 5 | 0.544 | $\alpha c/5$ | $c/5$ | $5R_c$ | $2\pi a_0/5$ | 0.2725 |

where: $E$ - is the electron energy, $V_{ax}$ - is the axial velocity, $V_t$ - is the tangential velocity of the rotating electron structure, $r_{mb}$ - is the value of the boundary electron magnetic radius in a plane normal to $V_{ax}$ vector, $c$ - is a light velocity, $R_c$ - is the Compton radius, $a_o$ - is the Bohr radius, $l_{ql}$ - is the trace length for a motion in closed loop (single quantum loop), $L_q$ - is the length size of the quantum loop as Hippoped curve with parameter $a = \sqrt{3}$.

The introduced parameter **subharmonic number** shows the rotational rate of the whole electron structure. The rotational rate decreases with the consecutive increase of this number, but the number of the first and second proper frequency cycles is not changed. This is very important feature formulated by the conclusion (B).

**(B) The number of first and second proper frequency cycles of the electron in closed loop with any subharmonic number is a constant.**

From the analysis provided in "Brief introduction to BSM theory"[4] it is evident that the electron makes 18778.362 rotations for one quantum loop. One quantum orbit may contain one ore more quantum loops. From Table 1 we see that for a confined moving electron the circumference length of the boundary of the electron's magnetic radius in a plane normal to $V_{ax}$ is equal to a whole number of $\lambda_c$

### 3.2. Quantum orbits. Emission and absorption of photon.

A stable quantum loop is defined by the repeatable motion of oscillating electron. The shape of such loop is defined by external conditions. Such conditions exist in the following simple cases:

- a quantum loop obtained between particles with equal but opposite charges and same mass, as in the case of positronium (see Chapter 3 of BSM)

- a quantum loop obtained between particles of opposite charges and different masses, as in case of the hydrogen atom.

In both cases the loops are repeatable and we may call them **quantum loops.** One or more quantum loops in series form a quantum orbit. It is usually a three dimensional closed curve. In case of hydrogen, any possible quantum orbits obtain a fixed position in respect to the proton.

The unveiled conditions of the electron motion in a quantum loop allow definition of any possible quantum orbit in the atoms and molecules. In Chapter 7 of BSM, the possible quantum orbits in Hydrogen are discussed and a model of Balmer series is suggested. Its analysis confirms the concept of confined motion of the electron. The trace length of the quantum orbit of Balmer series match the quantum loop No 2 from Table 1. The same quantum loop exists also in Deuteron. The BSM model of Hydrogen is different from the Bohr model, but all types of quantum numbers are identifiable. The quantum levels are obtainable by considering a whole number of Compton wavelengths but in a specific conditions defined by factors, such as the proximity distributed E-field of the proton, and its Intrinsic Gravitation field.

It appears that the limiting orbit has a length of $2\pi a_0$ and all other quantum orbits are inferior. This is valid not only for Balmer series in Hydrogen but also for all possible quantum orbits in different atoms, if they are able to provide line spectra. Therefore, the suggested physical model provides **a solution of the boundary conditions problem of the electron orbits for the Hydrogen and for all other atomic models suggested by BSM theory.**

The analysis of interactions between the oscillating electron in confined motion and oscillating CL nodes allows unveiling the process of the photon generation. According to the BSM concept, the emission of a photon, contributing to line spectra, is a result of **pumping of CL nodes** from the orbiting and simultaneously rotating and oscillating electron. In this process more than one orbital cycles are involved. **The emission of a photon occurs from the surrounding CL space in the moment when the electron drops from higher to lower energy orbit. This explains why the Quantum mechanical model needs an uncertainty principle, while the BSM model does not need such.**

In Quantum Mechanical models the CL substance is missing and the process of the photon generation has to be directly connected to the orbiting electron. In such case, it seems that the electron position could not be located, so a concept of "electron cloud" has been introduced. In BSM model the electron in the atom has well defined orbit, while the concept of CL space allow analysis of the electron motion in any portion of the orbit.

### 3.3 Lifetime of the orbital motion of the electron

In section 3.1 it was mentioned that the condition for phase repetition of the two proper frequencies of the electron with velocity $V = \alpha c$ (13.6 eV) are met for 2573380 electron turns (about 137 orbital cycles ) and approximately met for three orbital cycles. The full travel of the rotating electron in both cases can be expressed by the product of the number of turns and helical step. Taking into account the relativistic gamma correction the full travel is $(1/\alpha^3)\times s_e$. In the same time the quantum velocity of the electron is is known. Then dividing the full travel by the velocity we obtain the orbital lifetime.

$$\tau_{sp} = \frac{3\lambda_c}{\alpha^3 c\sqrt{1-\alpha^2}} = 6.248\times10^{-14} \text{ (s)} \qquad (7)$$

For a second harmonic quantum loops the number of electron turns is twice smaller, so its velocity and travel length are also twice smaller, so the lifetime appears the same. **Consequently the obtained equation (7) appears valid for a quantum orbit with any subharmonic number, *n*, comprised of single quantum loop as shown in Table 2**. It is quite reasonable to consider this to be the lifetime for spontaneous emission. For quantum orbit comprised of *m* number of quantum loops the lifetime will be *m* times larger. Such conditions appear for the higher order series of Hydrogen in respect to the Balmer series.

In case of simulated emission, the lifetime of the orbiting electron could be shortened. It is interesting to find what could be the shortest lifetime in which a photon generation is still possible. From Eq. [(3.43.h)] we see that this could be the lifetime corresponding to three orbital cycles. Proceeding in a similar way as for the spontaneous emission we arrive to the result

$$\tau_{min} = \frac{3\lambda_c}{\alpha^2 c\sqrt{1-\alpha^2}} = 4.5596\times10^{-16} \text{ (s)} \qquad (8)$$

Note: In the derived equations (7) and (8) the relativistic consideration are not taken into account.

**Summary:**

- The orbital lifetime for spontaneous emission is the time for which the first electron frequency makes 2573380 cycles
- The shorter lifetime for simulated emission is the time for which the first electron frequency make 18778.3 cycles (the secondary electron frequency makes 56335 cycles)

### 4. External shape and geometry of proton and neutron

The considerations leading to unveiling the structure and shape of the stable particles neutron and proton are given in the article "Brief introduction to BSM theory[4], while the detailed analysis is presented in the BSM theory. Both, the proton and the neutron are comprised by one and a same hardware compositions of helical structures, whose single turn element is the same as the electron structure. The proton and neutron are distinguished only by their external shape and the slight twisting difference in their helical structures that is responsible for their Newton's mass differences. The shapes of the proton and neutron are shown in Fig. 3.

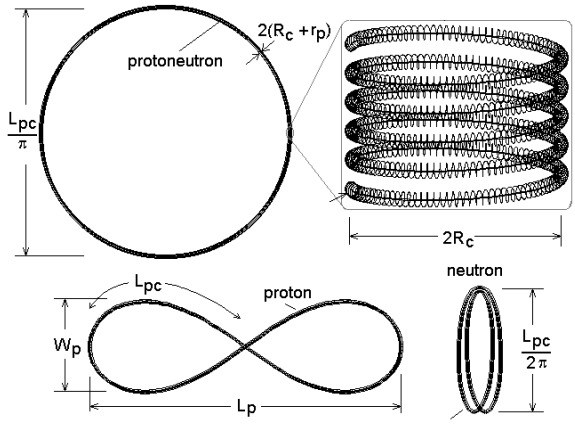


Fig. 3. Geometrical parameters of the proton and neutron. The magnified view shows only the external helical shell without the internal structures of pions and kaon (extraction from Atlas of ANS).

The proton is a twisted torus with a shape close to a figure 8, while the neutron is a same

structure but in shape of double folded torus. More accurately the plane projection of the proton envelope is quite close to a Hippoped curve with a parameter $a = \sqrt{3}$. The twisting (and folding) direction is strongly defined by the underlined structures of the pions and kaon inside the proton (neutron) envelope (see Chapter 6 of BSM). Consequently all protons (and neutrons) involved in the atomic nuclei have one and a same handedness.

The estimated geometrical parameters of the electron, proton and neutron are given in Table 2.

Physical dimensions of stable elementary particles Table 2

| Parameter | Value (m) | Description | Reference BSM Chapter No. |
|---|---|---|---|
| $L_{PC}$ | 1.6277E-10 | *p* and n core length | 5, 6 |
| $L_P$ | 0.667E-10 | *p* length | 6, 7, 8, 9 |
| $W_P$ | 0.19253E-10 | *p* width | 6, 7, 8, 9 |
| $r_e$ | 8.8428E-15 | small radius of $e^-$ | 3, 4, 6 |
| $r_p$ | 5.8952E-15 | small radius of $e^+$ | 3, 4, 6 |
| $s_e$ | 1.7706E-14 | $e^-$ ($e^+$) helix step | 3 |
| $R_c$ | 3.86159E-13 | $e^-$ Compton radius | Known |
| $2(R_c + r_p)$ | 7.8411E-13 | *p* and *n* thickness | 6, 7, 8, 9 |

Notations:
*p* - proton, *n* - neutron, $e^-$ - electron, $e^+$ - positron

The following question may arise: why the proton possesses a charge while the neutron - not. The answer is: The electrical charge is a result of the modulation of CL nodes by the internal lattice of the helical structures[4]. In case of neutron, all helical structures get overall symmetry in respect to its axis. For a such shape, the modulation of CL space in the far field is compensated and the electrical field is a zero. In case of proton, the overall torus is twisted and the axial symmetry of RL(T) is destroyed. Therefore, it is able to modulate the CL nodes also in the far field.

In fact the modulation symmetry for the neutron is not perfect in the near field as in the far field, so the neutron still exhibits some modulation of the CL nodes and consequently an electrical field, but only in a proximity range. This field is locked by the stronger IG field in the proximity range to its envelope so it is not detectable in the far field. The locking mechanism of IG field, although, does not work well when the neutron is in a confined motion in CL space, so it exhibits a magnetic moment (the magnetic moment of the neutron as a neutral particle has not been satisfactorily explained by the modern physics so far). The electrical field of the proton is always unlocked due to its different overall shape. Therefore, in the far range the electrical field of the proton appears as emerging from a point, but in the near field, it is distributed over the proton's envelop.

Fig 3 shows the spatial geometry of the Deuteron, where: *p* - is the proton and *n* - is the neutron. The neutron is centred over the proton saddle and kept by the Intrinsic Gravitation (IG) field and the proximity electrical fields of the neutron and proton. In such conditions the position of the neutron is stable with some rotational freedom, but it is not able to unfold and convert to proton.

Fig. 4 illustrates the protons and neutrons arrangement in the nucleus of He. In such close distance, the internal lattices of the proton's helical structures are kept by IG forces that are inverse proportional to the cube of the distance. The nucleus of helium is the most compact atomic structure. Therefore, its influence on the CL space parameters is the strongest one. As a result, the helium nucleus possesses the largest binding energy between the involved protons and neutrons.

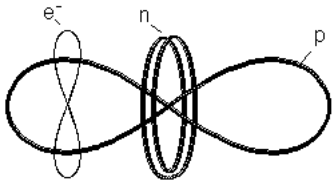


Fig. 4. Deuteron with electron in Balmer series according to BSM physical model

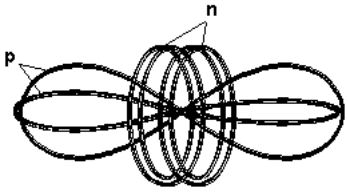


Fig. 5. Helium nucleus according to BSM physical model

When taking into account the two features of the proton: a finite geometrical size and the distributed proximity electrical field it is evident that the Coulomb law is valid down to some limit, defined by the finite size of the proton structure. This is verified by the model of Balmer series in Hydrogen

presented in Chapter 7. The idealized shape of Balmer series orbit is shown in Fig. [7.7].

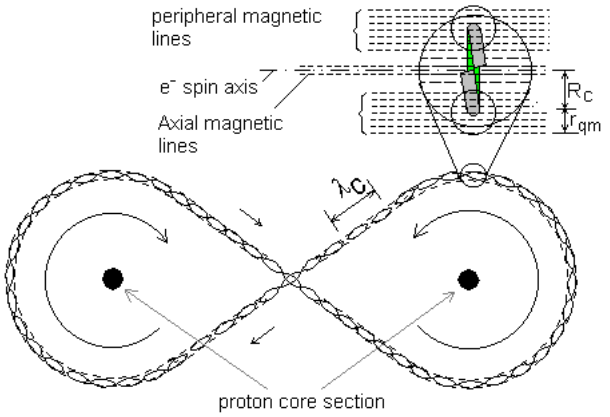


**Fig. [7.7]**. Idealized shape of Balmer series orbit. $R_C$ - is the Compton radius, $r_{qm}$ - is a magnetic radius of electron at sub optimal quantum velocity. The Compton wavelength $\lambda_c$ shown as standing waves is is not in scale

## 5. Atlas of Atomic Nuclear Structures

### 5.1. Physical atomic models according to BSM concept.

One of the most useful results of BSM theory with practical importance is the Atlas of Atomic Nuclear Structures[6,7] (ANS). The analysis leading to unveiling the spatial arrangement of the protons and neutrons in atomic nuclei is provided in Chapter 8 of BSM. It shows that the protons and neutrons follow a strict spatial order with well defined building tendency related to the Z number of the elements. The signature of this tendency matches quite well the row-column pattern of the Periodic table, the Hund's rules and the Pauli exclusion principle. The Atlas of ANS provides nuclear configurations of the elements from Hydrogen to Lawrencium (Z = 103). For drawing simplification of the nuclear structures, the protons and neutrons are presented by simplified patterns reminding their shape. The left part of Fig. 6 shows the patterns used for the proton, deuteron, tritii and helium, while the right part shows the most common shapes and possible dimension of the quantum orbits. The dimensions of the quantum orbits and the proton and neutron are given in one and a same scale.

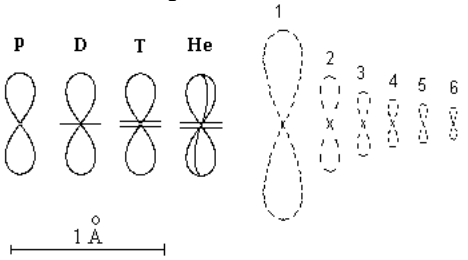


Fig. 6

Patterns for simple elements and quantum orbits

In the Atlas of ANS, the pattern of proton is symbolized by arrow in order to simplify the drawings. Additional symbols are also used for the same reason.

For any atomic nucleus, a polar axis can be identified. It is defined by the long symmetrical axis of one or more He nuclei in the middle of atomic nucleus. The atomic nuclei posses also twisting features due to the proton twisting, but it is not shown in the drawings. In the Atlas of ANS additional symbolic notations are used for the unveiled types of proton's bonds and pairing in which IG and EM fields are involved.

### 5.2. Three-dimensional structure of atomic nuclei and limited angular freedom of the valence protons.

The Atlas of Atomic Nuclear Structures provides the nuclear configurations of the stable isotopes. One or more He nuclei are in the nuclear centre, aligned with the polar axis of symmetry. The peripheral building blocks of the lighter elements are usually deuterons, while the element tritii appears more frequently in the nuclei of heavier elements. The positions of the protons are defined by the consecutive number of proton's shell and by the type of the bonds between the protons.

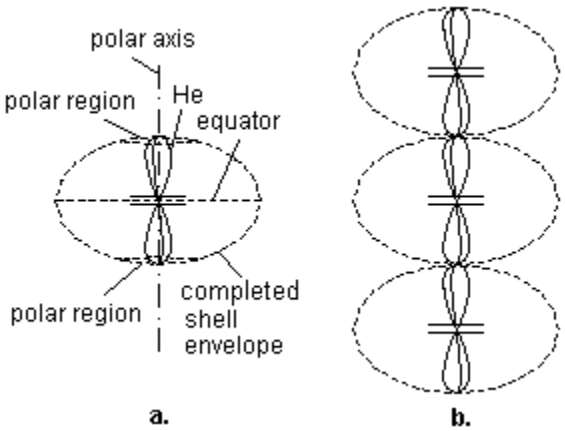


**Fig. [8.2]** a. - polar structure; b. - polar-chain structure

Fig [8.2] illustrates the backbone structure of nucleus allowing the most dens pack of the protons and neutrons, having in mind the repulsive forces

from the proximity fields of the protons. The polar chain structure appears for the atoms with Z > 18 (after Argon).

The unveiled type of bonds in the atomic nucleus are listed in Table 8.1.

**Bonds in the atomic nuclear structure** ***Table 8.1***

| Bond notation | Description |
|---|---|
| GB | Gravitational bond by IG forces |
| GBpa | polar attached GB |
| GBpc | polar clamped GB |
| GBclp | (proton) club proximity GB |
| GBnp | neutron to proton GB |
| EB | electronic bond (weak bond) |

The gravitational bonds are held by the IG field of the intrinsic matter (more explicitly the IG field of the internal lattices of the helical structures from which the proton and neutron are built). The IG field controls also the proximity E-field of the proton (and proximity locked E-field of neutron) and its unity charge appearance. For this reason, all GB types of bonds are very stable.

The four types of the gravitational bonds and one type of electronic bond are illustrated in Fig. [8.4], where the positions of some quantum orbits are also shown.

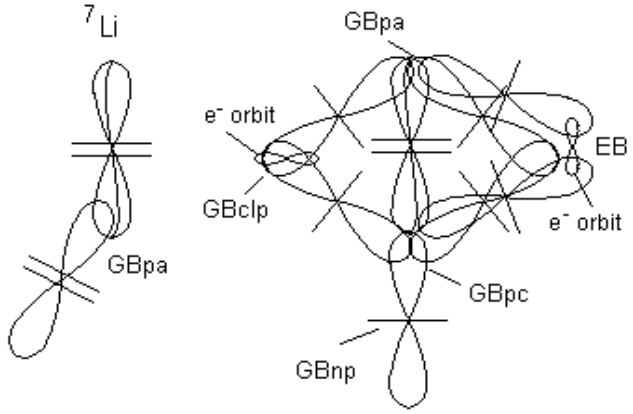


**Fig. [8.4]**
The left-side structure is $^{7}$Li nucleus,. The right-side structure is only a portion of nucleus showing the different type of bonds, according to Table [8.1]. The planes of the shown quantum orbits in fact are normal to the drawing plane

The GBpa and GBclp bonds can not have any freedom of motion. The GBpa bonds for valence protons have an angular restricted freedom of motion in a plane close to the polar section. The EB type of bonds are valid only for the valence protons but they are provided by electron orbit pairing, corresponding to the Hund rules. There are few types of such pairings. The two of them are more important: a first type - two orbits in separated parallel orbital planes; a second type - two electrons with different QM spins, according to a Pauli exclusion principle (their circling directions are opposite each other). The second type of Hund rule appears valid for EB bonds.

The structural restrictions of the positions of the atoms in the molecules comes from two factors:

- stable structural arrangements of the bonded protons of the nucleus

- angular restrictions of the valence protons.

The GB type bonds could not be broken in any type of chemical reaction, but only in nuclear reactions where quite large energies are involved. The EB type of bond however is weak. Bonds of such type begin from the raw 13 of the Periodic table while in raw 18 (noble gazes) they are converted to GBclp bonds. The EB bonds normally exclude the external shell protons from chemical valence, so they play a role for the principal valence of the elements from group 13 to 17. This is valid for rows 1, 2, 3 of the Periodical table. In some conditions, however, the EB bonds could be broken, so the element may exhibit multiple oxidation numbers.

For some chemical compounds between elements with large number of valence protons, not all free valence protons can be connected by electronic bonds. This is a result of the finite nuclear size of the atoms and the angular restriction of the valence protons.

It is evident from the nuclear structure that the positions of the electron orbits are strictly determined by the positions of the protons with their proximity electrical fields and the conditions of quantum orbits provided by Table 1. While the, the electron orbits are not shown in the Atlas of ANS, their positions are easily identifiable. It becomes apparent that: The first ionization potential, obtained experimentally and used in the Quantum Mechanical models of the atoms could be explained by the different positions of the electron quantum orbits in the atomic nuclei and the influ-

ence of the nuclear IG field (from protons and neutrons).

## 6. Electronic bonds between atoms in molecules

It is apparent that the BSM atomic models allows identification of the orbital planes and chemical bond orientation of the atoms in the chemical compounds. Additionally the quantum mechanical spin of the electron circling in orbit around the proton is also identifiable. The proton envelope is twisted torus, so it possesses a well-defined handedness along any one of its axes of symmetry. Then, the electron in the quantum orbit shown in Fig. 4 has an option to circle in two different direction in respect to the proton direction of twisting. This will corresponds to two slightly different energy levels. **Its signature is a fine structure splitting of the spectral line.**

The intrinsic conditions of the quantum orbits defined by the two proper frequencies of the electron and CL node dynamics are valid also for the bonding electrons in molecules. Let consider a most simple case of $H_2$ molecule identified as an ortho-I state. Its shape is illustrated in Fig. [(19.2)] In this figure the three-dimensional shape of the proton is replaced, for simplicity, by a 2-dimensional Hippoped curve with parameter $a = \sqrt{3}$. The molecular vibration in such simple system is of linear type. The long axes of the protons and quantum orbit are aligned with the molecular vibrational axis.

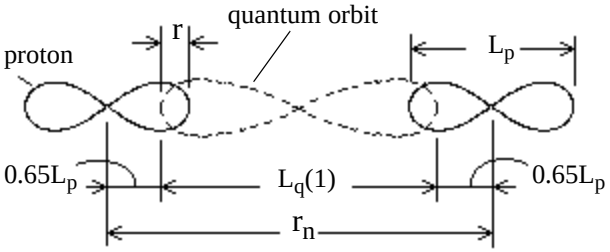


**Fig. [9.12]**
Structure of $H_2$ - ortho-I state molecule
$L_p$ - is a proton length
$L_q(1)$ is a long side of a first harmonic quantum orbit
$r_n$ - is the distance between the Hydrogen atoms
r - distance between the electron and the proton's core in the circular section (for the most external orbit
**Note:** The quantum orbit quasiplane is perpendicular to the quasiplane of the protons. However, they both are shown in one plane for simplification of the drawing

The both electrons circle in a common quantum loop (orbit) but in opposite directions (opposite QM spins). The quantum orbit crosses the Hippoped curves of the protons in the locus points. We may assume that every orbiting electron is able to neutralize one charge, by interconnecting its E-filed lines to the proton E-field. Let considering the moment, when both electron are in the locus points of the Hippoped curves, representing the protons. Their velocity vectors in this case are perpendicular to the direction of the molecular vibration and do not contribute to the momentum energy of the system. Then, their moment interaction can be estimated by considering only two unit charges at distance $r_n$. Now, let assume that the left proton and the right electron are both missing. The system energy in this case is $q/4\pi\varepsilon_o r_n$ [eV]. The same considerations and results are valid also for the other symmetrical case. Adding the energies from the two symmetrical cases we get the full system energy.

$$E = \frac{2q}{4\pi\varepsilon_0[L_q(1) + 0.6455L_p)]} = 16.06 \text{ eV} \qquad [(9.4)]$$

where: the factor 0.6455 defines the distance of the locus from the central symmetrical point of the Hippoped curve with factor $a = \sqrt{3}$.
The obtained value of 16.06 eV is pretty close to the experimentally measured vertical ionization potential of the photoelectron spectrum of $H_2$ (15.98 eV).

## 7. Vibrational motion of atoms connected in molecule by electronic bonds.

The Intrinsic Gravitation (IG) is important feature of the new concept about the vacuum. IG forces are involved in the following two cases

(a) strong attraction forces valid for small distances

(b) providing the energy of the electrical charge

The case (a) is valid not only for the prisms and nodes in empty space, but for elementary particles, atoms and molecules in CL space at small distances. Examples of the manifestation of the Intrinsic Gravitation are some of the Van der Wall forces between molecules and the Casimir forces between solid polished bodies in close proximity.

In case (b): BSM analysis unveils the physical meaning of the electrical charge as modulation of CL nodes by the IG field of the internal RL structures of the helical structures from which the particles are built[4]. In such aspect the energy of the electrical charge could be regarded as a part of the IG energy of the particle in CL space environment. The proximity field of the charge (in approximate range in order of Bohr radius) possesses a spatial configuration, while it appears as a point charge in the far field. The study of vibrational motion of two atoms connected in molecule by electronic bonds unveils one important feature. The vibration causes spatial modulation of the near electrical field created by the protons involved in the electronic bond. This feature is analysed by using a total energy of the system that includes:

- the IG energy
- the energy of the electrical charge
- the kinetic energy of the involved particles
- the energy of the emitted or absorbed photon
- the vibrational energy

The energy of the IG field is presented as an integration of IG forces from some initial value to infinity, but practically the integration could be truncated at finite distance because the IG field falls too fast with the distance

$$E_{IG}(CP) = -2\int_{r_{ne}}^{\infty}\frac{G_o m_{po}^2}{r^3}dr = \frac{C_{IG}}{(L_q(1)+0.6455L_p)^2} \qquad [(9.13)]$$

where: $m_{po}$ is the Intrinsic mass of the proton, $G_o$ is the intrinsic gravitational constant

$C_{IG} = G_o m_{po}^2$ - IG factor

***Note***: The factor 2 in front of the integral comes from the two arm branches (along *abcd* axes) of the CL space cell unit. They both are included in the *xyz* cell unit to which all the CL space parameters are referenced. All equations using $C_{IG}$ factor in the following analysis confirms the need of factor 2.

The principle of energy conservation is universally valid. The new concept, however, allows to see that the IG energy balance is quite fast. This means that the momentary total energy balance should be investigated. Based on this approach the vibrational motion of the most simple diatomic molecule $H_2$ (shown in Fig. [9.12]) is analysed.

The total momentum energy balance at the equilibrium point is given by

$$\frac{C_{IG}}{q(L_q(1)+06455L_p)^2} = \frac{2E_q}{q}+\frac{2E_K}{q}\ \text{(eV)} \qquad [(9.18)]$$

where: $2E_q/q = 511$ KeV - is the energy of the two electrical charges (for two protons); $2E_K/q = 2 \times 13.6$ eV - is the kinetic energy of the two electrons.

The analysis unveils the vibrational states and one metastable state of $H_2$ ortho-I molecule. For the vibrational levels with good for identification accuracy, the following expression is obtained:

$$E_\upsilon = \frac{C_{IG}}{qr^2}-\frac{2E_q}{q}-\frac{2E_K}{q}+6.26\ \text{(eV)} \qquad (9.23)$$

$$r = [[L_q(1)](1-\pi\alpha^4(\upsilon_m-\upsilon)^2)]+0.6455L_p \qquad (9.23.a)$$

where: v - is the vibrational level, $v_{max}$ is the max vibrational level identified by the photoelectron spectrum.

The small value of 6.26 ev in Eq. (9.23) is likely a constant due to integration in Eq. (9.13) and its value is obtained by fitting the calculated vibrational levels to identified optical transitions.

The photoelectron and optical spectrum are analysed and the corresponding transitions and vibrational levels are identified. The calculated vibrational levels are compared to the identified vibrational levels from the optical spectrum. The dependence of the vibrational levels from vibrational quantum number fits quite well after adjusting one small energy value that is a constant from integration in Eq. [(9.13)] This value, however, is about 10E-6 time smaller in comparison to the IG energy and could be omitted. Therefore, the analysis allows to determine the important parameter $C_{IG}$.

$$C_{IG} = (2h\nu_c + h\nu_c\alpha^2)(L_q(1)+0.6455)L_p) \qquad [(9.17)]$$

$$C_{IG} = G_0 m_{n0}^2 = 5.2651\times10^{-33}$$

**Any disturbance of this balance is related with emission or absorption of a photon. This is an important conclusion from the analysis.**

Fig. [9.24] shows the energy levels $E_v$, calculated by Eq. [(9.23)] and vibrational levels of the optical transitions E(0-ν'') and E(1-ν'') taken from experimental data[8] (I. Dabrowsky, 1984). The op-

tical spectrum is from a $H_2$ system known as a Lyman system.

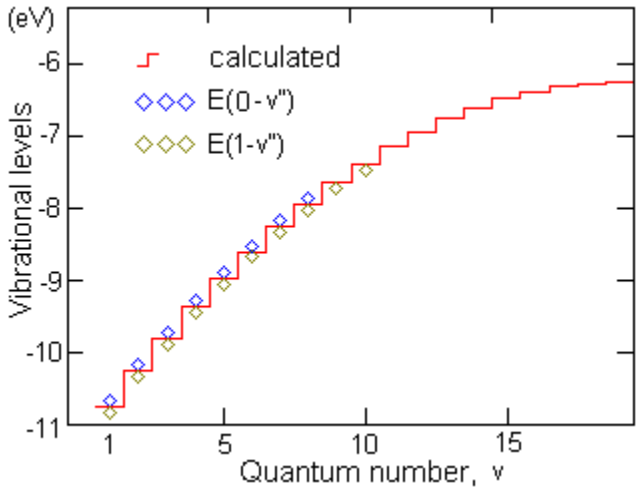


**Fig. [9.24]**. Energy levels $E_v$, (eV) calculated by Eq. (9.23) and vibrational levels of the optical transitions E(0-v'') and E(1-v''), corresponding to two QM spin values. The calculated levels are shown by step line, while the optical transitions by diamonds.

The shown vibrational levels corresponds to optical spectrum in UV range. They are result of transitions between these levels (including other "rotational levels") and one metastable state of $H_2$ molecule, the physical configuration of which is unveiled (discussed in Chapter 9).

The fractional error between the calculated levels ($E_v$) by Eq. [(9.230] and the optical data is within +/- 0.035%.

Similar analysis is provided also for $D_2$ molecule since it is a more typical building element in the atomic nuclei. Applying further analysis for diatomic molecules an analytical expression for vibrational levels, $\Delta E$ of homonuclear molecules is obtained, allowing a determination of the approximate internuclear distance of a homonuclear diatomic molecule.

$$r_n(n, A, p) = (A - p)\sqrt{\frac{2\alpha C_{IG}}{pE_B(n)}} \qquad (9)$$

where: EB(n) is the momentum total balance energy of the electronic bond given by Eq. (9.23), *A* - is the atomic mass of participated atom in mass units, *n* - is the subharmonic number of the quantum orbit, *p* - is the number of connected protons (valence number)

The conditions defining the intermolecular quantum orbits are different from those of atomic quantum orbits. For atomic orbits, the definition conditions are referenced to the home nucleus and not influenced by another nucleus. For intermolecular quantum orbits, however, the definition conditions are influenced by the nuclear motion of involved atoms, in which the IG field interactions are also involved. The IG forces are able to modulate the spatial configuration of the proximity E-field of the protons involved in the chemical bond. **As a result, the vibrational quantum conditions occur at intrinsically small deviations from the internuclear distance (see Chapter 9).** For $H_2$ ortho-I molecule, for example, the vibrational range is only 4E-16 (m) while the internuclear distance is 2.23E-10 (m). This effect in fact facilitates the identification of the possible configuration of a simple molecule by combination of two methods: an internuclear distance calculation and a drawing method[4]. The second one is based on the physical dimensions of the proton (and neutron) and the possible quantum orbit.

## 8. Combined method for determination of the possible configuration for diatomic molecules

The possible molecular configurations of a diatomic molecule can be unveiled by using the following approach:

- a drawing method: using the spatial configuration of the involved nuclei and a selected possible orbit from the quantum orbit set
- a theoretical calculation of the corresponding internuclear distance by Eq. (9).
- matching the calculated data with identified spectral bands from the optical and photoelectron spectra.

Examples of using the above approach are shown in the article Brief introduction to BSM theory[4]. Some of results for diatomic molecules are shown in Fig. [9.43], [9.45], [9.54], [9.56]. In these drawings the protons and neutrons in the central polar section of the atomic nucleus are only shown.

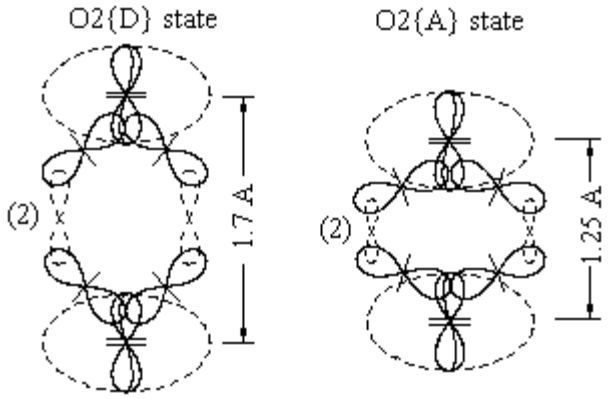


**Fig. [9.43]** Possible configurations of $O_2$ molecule in different states (D) and $O_2$(A). (structural states {D} and {A} denoted by BSM model?). The orbital planes of electrons do not lie in the drawing plane, but they are shown in this way for drawing simplification. The number in a bracket indicates the subharmonic number of the quantum orbit.

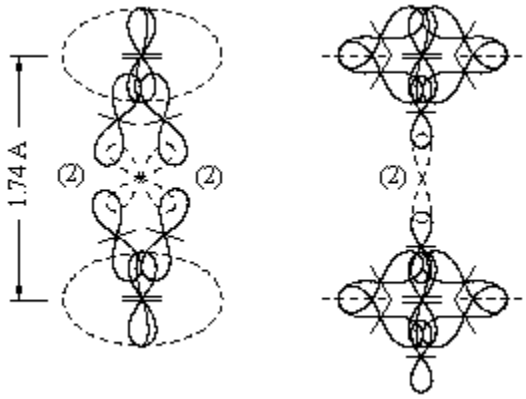


**Fig. [9.45]** A possible configuration of $O_2$ molecule in {E} state

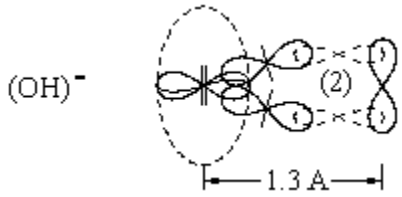


**Fig. [9.54]** Configuration of $(OH)^-$ ion. Every electronic bond orbit contains two electrons with opposite QM spins (the planes of bonding orbits are at 90 deg, in respect to the protons equivalent planes)

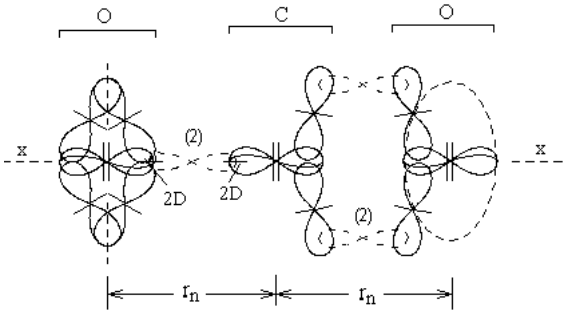


**Fig. 9.56** One view of $CO_2$ molecule. The CO2 molecule possesses rotational symmetry about the polar axis due to the 90 deg rotational symmetry of C atom. If rotating 90 deg around zz axis the view of the left side will change with the view of the right side.

.

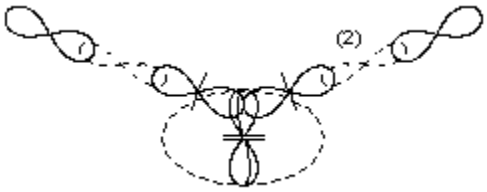


**Fig. [9.59]** Water molecule

## 9. Structural and angular restrictions of the chemical bonds of electronic type

### 9.1. Restrictions imposed by the nuclear configuration of the involved atoms

The provided considerations in §5, §6 and §7 demonstrate that the structural and angular restrictions reduce significantly the degree of freedom of the atoms connected by electronic bonds. The same restrictions are also responsible for the molecular bending. These restricting features are not apparent from the Quantum mechanical models of the atoms.

The mentioned considerations are not valid for ionic bonds where the atoms are not connected by electronic bonds but by attractive forces between oppositely charged ions. The internuclear distances in ionic bonds are also larger and such molecules exhibit different physical properties. Consequently they are not able to possess vibrational motion in which the quantum orbits play important roles. For this reasons the ionic compounds don't have vibrational rotational spectra. Only separated ions are able to provide ionic line spectra.

The following conclusion is valid only for chemical compounds with electronic bonds, but not for compounds with ionic bonds.

- **The degrees of freedom of connected atoms in molecules by electronic bonds are reduced by structural restrictions and limited angular freedom of the valence protons. This restrictions are defined by the nuclear configurations of the involved atoms.**

### 9.2. Restrictions from spin-orbital interactions

If not taking into account the implemented He nucleus in the atomic nucleus and the polar electrons, every single proton in the nucleus has own electron, connected to the free club of the proton (one that is not polar attached). Some of these proton's clubs, however, are GBclp or EB bonded in pairs. For EB bonded protons the two electrons with opposite QM spins circulate in a common orbit whose plane is almost parallel to the polar atomic axis. For GBclp bonded protons the two electrons with opposite spins circulate in a common orbit whose plane is almost perpendicular to the polar axis. In both cases, the common quantum orbit passes through the clubs of the protons. The orbital trajectory is well defined by the proximity E-field of the involved protons. The positions of GBclp protons are strongly fixed, while the EB protons are weakly fixed by the quantum orbits. Any fixed orbit may not lye in a plane but it is quite close to a fixed equivalent orbital plane that gets a proper symmetrical position in respect to the polar nuclear axis. From above mentioned consideration it is evident that the quantum orbits connected to BGps, GBclp and EB type of bonds have fixed orientation of their equivalent planes. These fixed positions are held much stronger than the orbital plane positions of the chemical bonds.

Table 2 provides the number of different type proton bonds in the nuclei of some elements and the total electrons with commonly aligned equivalent orbital planes.

Table 2.

| Atom | GBclp | EB | $N_e$ |
|---|---|---|---|
| C | 0 | 0 | 2 |
| N | 0 | 1 | 2 |
| O | 2 | 0 | 6 |
| P | 4 | 1 | 10 |
| S | 4 | 2 | 10 |
| Cl | 4 | 3 | 10 |
| Ca | 8 | 0 | 18 |
| Fe | 8 | 0 | 18 |
| Cu | 8 | 4 | 18 |

where: $N_e$ - is the number of electrons with aligned equivalent orbital planes.

In the analysis provided in Chapter 8 and 9 of BSM it is found that two of the external shell protons of the oxygen atom are GBclp bonded. The signature indicating such type of bonding appears in the first ionization potential trend as a function of Z-number and also in the photoionization potential of the oxygen (known as autoionization feature). The nuclear structure of Oxygen is illustrated in Fig. 7.

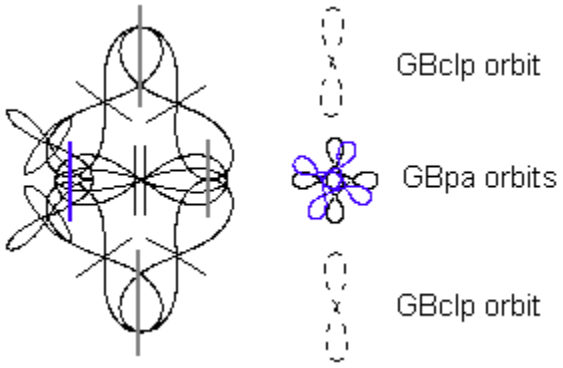


Fig. 7. Nuclear structure of the Oxygen atom

In the right part of the drawing, the common positions of the fixed electron orbits are shown as viewed from the polar axis. The projections patterns of the two polar orbit electrons (1s electrons according to QM model) are shown by different colours. Their similar patterns exhibit a small angular displacement around the polar axis due to the twisting of the atomic nucleus. This feature, valid for all atoms, is a result of the proton twisting. The GBclp bonded protons (deuterons) are shown in the plane of drawing, while the valence protons (deuterons) are closely aligned to a perpendicular plane,

but shown at oblique angles for a drawing simplification purpose.

The stability of such nuclear configuration with two GBclp pairs is evidently a result of the nuclear symmetry in which the two polar electrons (from 1s shell) have strong influence. This configuration provides much larger angular freedom of the two valence protons that may explain the large chemical activity of the Oxygen atom.

## 10. Application of the BSM models for analysis of biomolecules with identified structure and composition.

### 10.1. General considerations

The 3D structures and atomic compositions of many biomolecules now are well known. In such structures, the individual atoms are identified as nodes with known coordinates. The angular coordinates of their chemical bonds are also known. This information is sufficient to allow a replacement of the nodes in the 3D structure of any large molecule with the physical models of the atoms according to the BSM theory. If the BSM atomic models are correct, their three-dimensional structure and angular bond restrictions should match the three-dimensional structure of the biomolecules. Once the BSM models are validated and corrected if necessary, the properties of the complex biomolecules and any macromolecule with known shape could be studied and analysed from a new point of view. The application of the BSM models, for example, allows an identification of the positions of all orbits. This includes the internal shell and the chemical bonds electronic orbits, as well. The conditions for possible interactions, modifications and energy transfer could be analysed at atomic level.

### 10.2. Ring atomic structures in organic molecules.

Most of the organic molecules contain ring atomic structures. The molecule of benzene could be considered as a simple example of a ring structure. The biomolecules usually possess a large number of ring atomic structures. Fig. 8. shows the 3D molecular structure of aspirin where the ring structure of 6 carbon atoms is similar as in benzene.

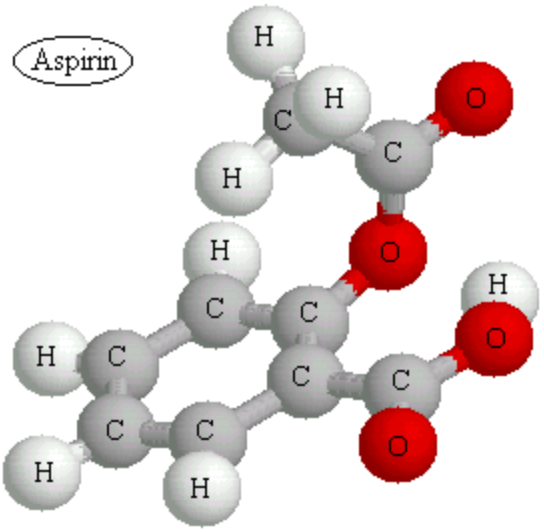


Fig. 8
3D structure of the molecule of aspirin (PDB file aspirin visualized by Chime software)

Fig. 9 shows the same structure of aspirin at atomic level by application of BSM atomic models.

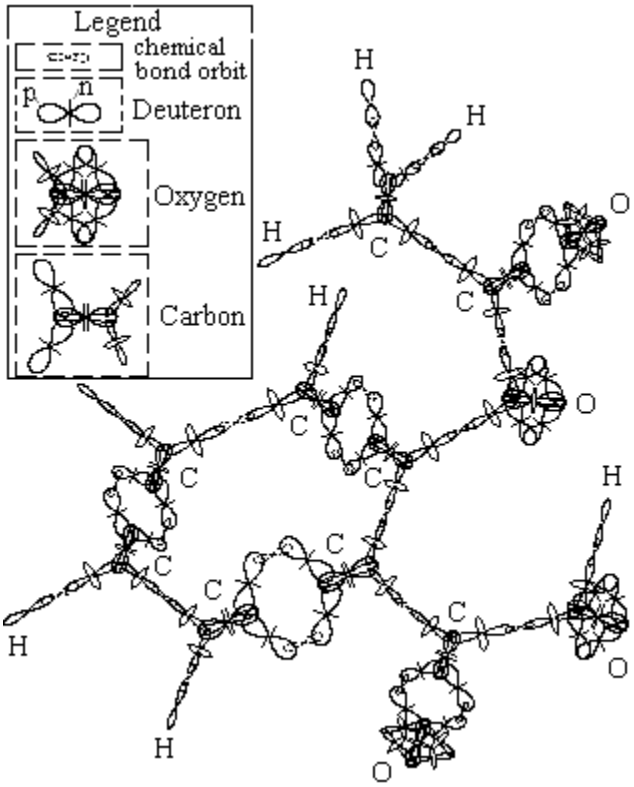


**Fig. 9** 3D structure of aspirin by BSM atomic models

The single atoms Deuteron, Oxygen and Carbon and the size of quantum orbit of second subhar-

monic are shown in the left upper corner. The valence protons (deuterons) of the oxygen atom are in fact in a plane perpendicular to the plane of EB bonded protons (deuterons) but they are shown with reduced dimensions in order to imitate an oblique angle in a 3D view. The same is valid also for the valence protons of the carbon atom.

In Fig. 9 the electronic orbits providing chemical bonds are only shown. For molecule with known 3D structure and composition the common positions of all electronic orbits with their equivalent orbital planes are identifiable. It is clearly apparent that the 3D structure of the molecule is defined by the following conditions:

(a) a finite size of the involved atomic nuclei

(b) an angular restricted freedom of valence protons

(c) a finite orbital trace length defined by the quantum conditions of the orbiting electron

(d) orbital interactions

(e) a QM spin of the electron (the motion direction of the electron in respect to the proton twisting)

The QM mechanical models of atoms are mathematical models in which the features (c), (d), and (e) are directly involved, while the features (a) and (b) are indirectly involved by the selection of proper wavefunctions. In this process however some of the spatial and almost all angular restrictions are lost. Let emphasize now the difference between the suggested BSM models of atoms and molecules from one side and and the QM models from the other.

- QM model: the electrons participating in chemical bonds are orbiting around both point-like nuclei, i. e. they are not localised between the nuclei

- BSM model: the electrons involved in the chemical bonds are localised between the nuclei

-QM model: the chemical bond lengths are estimated from the electron microscopy assuming the planetary atomic model in which the larger electron concentrations are centred around the poinlike nucleus

- BSM model: the chemical bond length may need re-estimation, because the orbits of the chemical bond electrons do not encircle the bound atomic nuclei.

- QM model: The length of C=C double valence bond is estimated as 1.34 A (angstrom), while for a single valence C-C - as 1.54 A. However, these lengths show a small variation in the same ring groups included in different biomolecules.

- BSM model: the length of single C-C bond may vary only by the subharmonic number of quantum orbit, while the length in a double C=C bond is additionally dependent of the angular positions of the valence protons.

The adopted and existed so far concept of circling delocalised electrons for explanation of the equality between single and double bonds in benzene molecule is not logical from a point of view of BSM model. This is quite important for unveiling some of the specific properties of the ring structures in the biomolecules.

Ring structures are very abundant in many biomolecules and they are very often arranged in particular order along the long chain structure of the molecule. DNA and proteins contain large number of ring structures. Fig. 10 shows the spatial arrangement of ring atomic structures in a portion of β–type DNA. The positions of some (O+4C) rings from the deoxyribose molecule that is involved in the helical backbone strands of DNA are pointed by arrows.

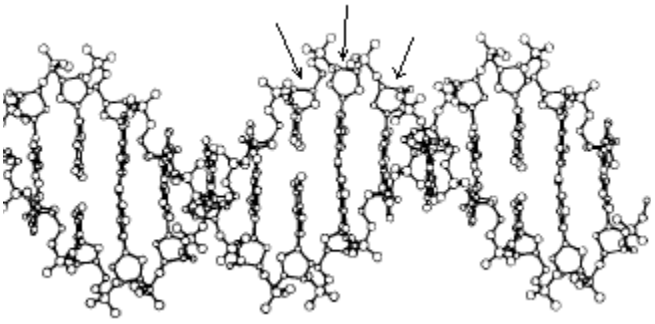

**Fig. 10** Part of DNA structure with indicated positions of some of (O+5C) atomic rings

Fig 11. shows the ring atomic structure (O+4C) from the DNA strand. The deuterons involved in the ring structure shown in Fig. 11 practically have some small twisting, but the quantum orbit of single valence bond also could be twisted. This feature gives some freedom for formation of ring structures of different atoms. The rotational freedom of the single valence bonds, however, may

be accompanied by some stiffness that increases with the degree of the orbital twisting.

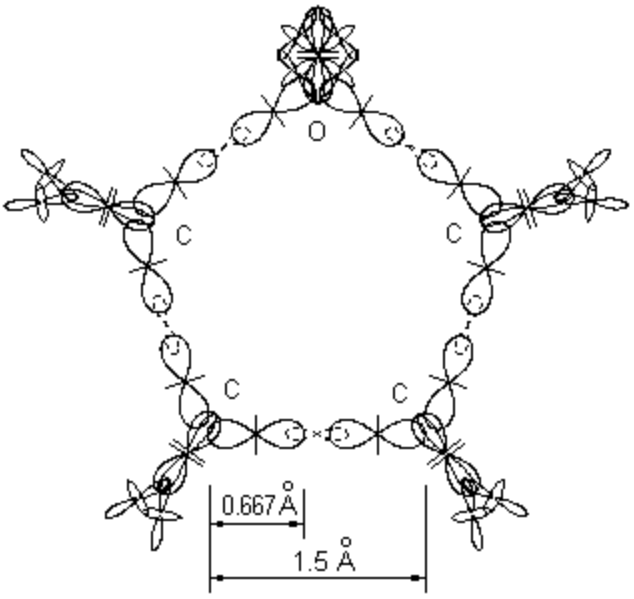


**Fig. 11.** Ring atomic structure from the deoxyribose molecule involved in DNA strand

In DNA molecule, some of the atoms of the ring structure are also connected to other external atoms. All this considerations provide explanation why the ring structure (O+5C) connected to the DNA strand is not flat but curved.

### 10.3 Weak hydrogen bonds

It is known that a weak hydrogen bond is possible between two atoms, one of which does not possess a free valence. The bond connection is a result of orbital interactions. In such aspects, the hydrogen bonds connecting the purines to pyramidines in DNA molecule are of two types: <N-H...O> and <N-H...N>, where the single valence electronic bond is denoted by "-" and the H-bond is denoted by "...". The BSM concept allows to find the possible orbital orientation for such type of bond. This is illustrated by Fig. 12.

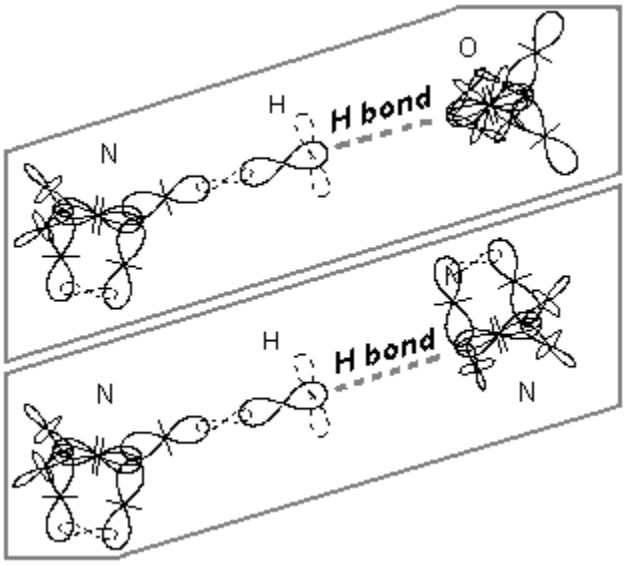


**Fig. 12**. Two types of hydrogen bonds

In a hydrogen bond of type N-H...O the plane of electronic orbit of hydrogen appears almost parallel to the commonly oriented nuclear orbits of oxygen atom in which six electrons are involved (see Table 2 and Fig. 6). In a hydrogen bond of type N-H...N the plane of electronic orbit of hydrogen is almost parallel to the equivalent planes of the two polar orbits of N in which two electrons are involved.

It is evident that the hydrogen bond is characterized by the following features:

- the connection is a result of common orbital orientation
- the H-bond requires critical range of distance
- the H-bond allows a rotational freedom in a limited angular range.

This three features allows the DNA molecule to possess excellent folding properties.

### 10.4. Hypothesis of energy storage mechanism in molecules possessing ring atomic structures.

It is well known from the atomic spectra, that only the alkali metals (Group I) and the positive atomic ions with a single valence electron possess atomic spectrum that could be described by the Bohr atomic model. For elements with more than one valence electron, the principal quantum numbers exhibit more than one energy level (degenerate levels), due to the spin orbital interactions. The

signature of this feature is apparent from the Grotrian diagrams of the atomic spectra. The spin-orbital interaction from a point view of BSM atomic models is discussed in Chapter 8 of BSM. The analysis leads to a conclusion that the pumped CL space energy is not emitted in full, after an orbiting electron is dropped to a lower quantum level. Part of the pumped energy is preserved by the atomic nucleus and redirected to the valence proton, whose quantum orbital plane is parallel to the orbital plane of the consideration. The physics of this effect is explainable if considering the total energy balance including IG field. The latter controls the proton's proximity E-fields distribution, that from his hand defines the orbital conditions of the electron. Therefore, the redirected energy provides some shift of the energy levels, but the effect is stronger for the lower states, closer to the ground state of the series (Balmer series has own ground state, according to BSM model). The physical explanation of this effect allows making a conclusion that the released energy prior to formation of a photon is **preferentially guided by connected structures of protons (deuterons)**. Applying the same considerations for the ring atomic structures there must therefore be a guiding energy process between the atomic nuclei or protons involved in the ring. Such consideration leads to the following conclusion:

**In proper environments, the ring atomic structures in organic molecules may have ability to store energy as an exited state rotating in the ring loop.**

The effect of the rotating excited state is possible due to the consecutive re-excitation of the electrons in the separate bonding orbits in the ring. This effect is not apparent by the Quantum mechanical model, where the wavefunctions are complex envelope around the whole nuclei of the involved atoms. However, it is a known fact that the bonding strengths between atoms involved in a ring atomic structure are stronger than between same atoms when not participating in such structure.

Evidently, the condition of rotating excited state in a ring structure could be obtained only for equal energy level differences. Such concept allows considering excited states not only from same valence bonds but also from single and second valence bonds as well. From the other side, for a ring structure containing more than two bonds of same valence, excited states may preferentially exists between the same valence bonds. In case of aspirin, for example, such conditions exists for three pairs of orbits of second valence and three pairs of orbits of single valence bonds. If considering also the fixed nuclear orbits of the atoms in the ring then twelve polar electrons could be also involved in a ring storage effect. Theoretically they may store a much larger energy not only due to their number, but also due to the larger transition energies.

In proper environments, the stored energy in the ring structures of the biomolecules may have the following features:

**- a stable cycle of exited state rotation due to a stable finite time of single excited state**

**- a possibility for interactions with properly oriented neighbouring ring structures in the moment between two consecutive excited states (conditions for synchronization between the rotating states of neighbouring rings)**

**- a cascade type of energy transfer**

Many of the building blocks of the biomolecules or reagents contain number of single or attached rings. For example Adenine (2 attached rings), Guanine (2 attached rings). Vitamin D contains one single and two attached rings. Alpha and Beta tubulins contain groups of: GDP (one single and two attached rings), GTP (one single and two attached rings), TAXOL (4 single rings). The steroids hormones contain usually four attached atomic rings. The ATP, an important energy carrier in the cells contains one single and two attached rings. It is quite logical to consider that the energy rotating cycles in the attached rings are mutually dependable so they must be synchronized. Then it is logically to expect that the attached rings may have an increased ability to hold a stored energy in case of environment change.

## 10.5 Hypothesis of energy flow through the chain structure of the biomolecule.

### 10.5.1. Energy flow in DNA molecule and its effect on the higher order structural characteristics.

For long chain biomolecules, like DNA, the ring atomic structures are characterised by few additional features:

(a) a strong repeating order

(b) a strong orientation in respect to the host strand of DNA

(c) a strong orientational order of the neighbouring rings along the helix

These features are well known and can be easily visualized when rotating the 3D structure of DNA (by programs like: “chime” “Rasmol”, “protein explorer” etc.).

The consideration of cascade type of excited state transfer could be applied not only for a ring atomic structure but also for a long chain molecule built of repeatable atomic structures connected by electronic bonds. In this case some more complicated but mutually dependable mechanisms are involved. The following analysis tries to unveil such mechanisms. Let considering for this purpose one of the backbone strands of DNA. Fig. 13. illustrates the connection path of the electronic bonds in the strand.

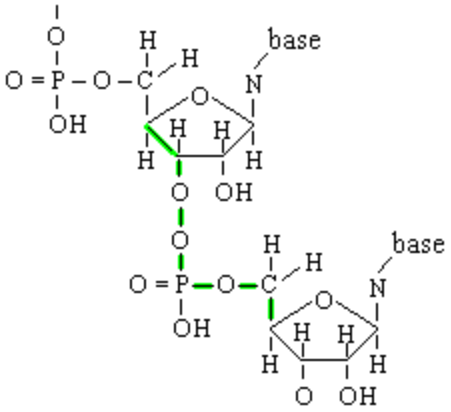


**Fig. 13**. Bond connection path through a DNA strand
The connection path corresponding to one cascade of the nucleotide is denoted by a thick green line

Three important features are apparent for every repeatable cascade:

(d) the bond connection path is formed by deuterons or protons connected by electronic orbits

(e) the bond connection path passes through one C-C bond from the (O+5C) ring.

(f) all bonds involved in the bond connection path are single valence

It is reasonable to expect that the long chain of single valence bonds may provide conditions for cascade excited state transfer in one direction. The time of every excited state is determined by a quantum mechanical consideration - the lifetime of the spontaneous emission. Having in mind the small distance between the neighbouring electronic bonds, the transfer time between two consecutive excited states (with a light velocity) is practically almost a zero. Then the time dependence between the two energy process (a cascade energy transfer and cycle period of energy rotation in the ring) is easily obtainable. The bonding path of one cascade contains six bonds total in which one C-C bond from the (O+4C) ring is included. This ring involves five bonds. Then one may consider that the following condition is valid:

$$0 < (T_R - t_c) < \tau_{av} \qquad (9)$$

where: $t_c$ - is the time transfer interval for one cascades of nucleotide estimated by the sum of lifetimes of excited states in involved bonds, $T_R$ - is the cycle time of the rotating state in the ring, $\tau_{av}$ - is the average lifetime for a single bond.

The expression (9) means that the cascade transfer and ring cycle are mutually time dependable processes, so they should have proper **phase synchronization.** Additionally, all parameters of Eq. (9) are dependable from the temperature, but in a different way. This will impose a limit temperature range for successful phase synchronization.

Keeping in mind the features (a), (b), and (c), the rotating energy states in the ring could be commonly dependable.

The whole mechanism will be characterised by the following features:

(k) the rotated excited states in (O+5C) rings will possess one and a same handedness determined by the direction of cascade energy flow through the strand to which they are attached

(l) the rotating energy states are phase synchronized along the DNA strand

(m) the rotating energy states sustain the tendency of unidirectional cascade energy flow through the DNA strand

(j) the whole mechanism will work at optimum temperature and limited temperature range both defined by the conditions of optimal phase between the cascade energy transfer and the ring energy cycle.

It is apparent that the commonly dependable features (g), (h), (h) and (j) will lead to a self-sustainable mechanism.

Let analyse now the conditions that may support the tendency of unidirectional energy transfer. For this reason we will consider a small portion of DNA ignoring it supercoiling. In such case it could be regarded as a linear type DNA. It is important to emphasize two structural features of Beta type DNA that might be related to the tendency of unidirectional energy transfer:

- It is well known that the nucleotide arrangement in DNA is antiparallel, so the same definition is valid, also, for the bonding paths through the two strands.

- The DNA double helix is characterised by a minor and major grove. This means that one of the helix is slightly axially shifted in respect to the other.

The concept of unidirectional energy flow through the DNA strand could be investigated if associating it with the magnetic field of a solenoid. In such approach, the double helix configuration of DNA could be regarded as two parallel solenoids with a common axis. Now let consider that the cascade energy flows through the both strands are in opposite (aniparallel) directions. This will corresponds to opposite currents through both solenoids. In such case, the magnetic lines in the internal region of the solenoids will have antiparallel direction, while the external magnetic lines will be closed in the proximity of both ends of the solenoids.

Let call this type of field a "**complimentary compensated solenoids type**". The magnetic lines of such field are schematically illustrated by Fig. 14. The two solenoids that simulate the two strands are shown by green and red. Their field lines shown as dashed lines are antiparallel inside the solenoids, while they are connected in proximity at the both ends.

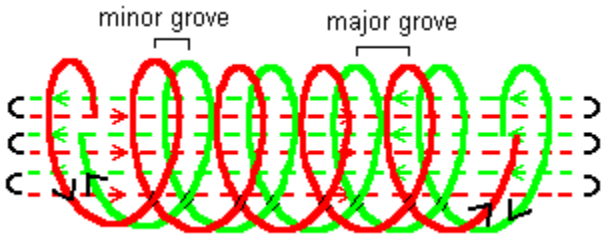


**Fig. 15.** Association of energy flow conditions between DNA strands with complimentary compensated solenoids. The magnetic field lines close in a proximity at both ends of the solenoids. The current directions in both solenoids are opposite (shown by black arrows)

If attempting to separate the both solenoids, they will opposed.

The analysis of magnetic field with such spatial configuration leads to the following additional features:

(h) The configuration of the associated magnetic field is independent of the secondary (supercoiling) shape of DNA

(i) Such type of magnetic field will provide an additional strength of the connections between the both strands. It will oppose the separation between the strands because this leads to increase of the close path lengths of the magnetic lines

(j) For a small portion of DNA molecule the complimentary compensated solenoids type of field is axially symmetrical.

The provided considerations may put also a light about the hydrophobic mechanism existing in the space between the two DNA strands. The two bond angles of the water molecule are illustrated in Fig. [9.59] where the positions of the orbits of the two valence electrons are also shown. If a water molecule is placed inside the symmetrical field of the compensated solenoids, the angular positions of the valence electron orbits evidently will be in a conflict with the solenoids field. The interaction of the orbiting electrons with such field may provide expelling forces for such type of molecule. This might explain the hydrophobic environments of the internal region of DNA between the two strands. The hydrophobic environment is quite important for H-bondings between the purines and pyrimidines.

The analysis of compensated double solenoid model for the energy flow through DNA leads to the following conclusion:

**(A). The DNA double helix molecule could be easily folded in any shape under influence of external factors.**

The external factors could be different kind of proteins.

### 10.5.2. Magnetic field conditions for proteins.

It is well known, that in proper environments the proteins, possessing usually a complex tertiary structure, preserve their native shape. The linear DNA, from the other side, when it is free of bending proteins, does not exhibit such a feature. The main reason for the different behaviours of the proteins and the DNA of linear type perhaps is a result of the structural differences between them. The protein is a long single strand molecular chain with diversified sequences of aminoacids. The protein backbone does not contain low order repeatable structures as the DNA nucleotide. It may contain, however, higher order repeats, that may form some helices with small number of turns or other spatial configurations. In such arrangement the conditions for H-bonding are significantly reduced. All these structural differences indicate that we could not apply the concept of the complimentary compensated solenoids for the proteins, as for the analysis of DNA.

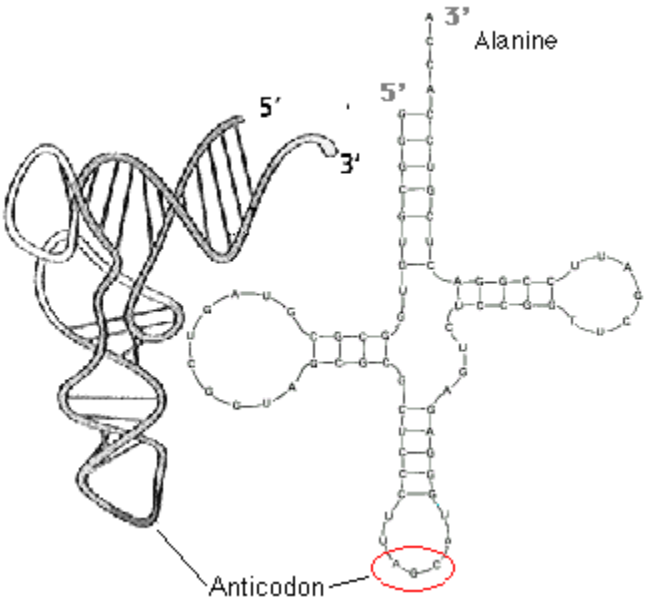


**Fig. 16.** tRNA molecule. (a) - real shape, (b) plane drawing, showing the loops and base pairs

The conclusion, that the diversified sequence of the aminoacids is one of the reason for the different higher order shape of the proteins is supported by the analysis of the shape of the tRNA molecule. Its shape and atomic composition is shown in Fig. 16.

The tRNA molecule possesses a single strand of base pairs but the repeating order of the nucleotides is similar as in the DNA molecule. Its single strand arrangement obtains a stable shape of "cloverleaf" demonstrating in such way a tendency for arranging parts of the long single strand in proximity.

In such arrangement, the unidirectional magnetic field through the single chain of tRNA becomes closer to the magnetic field of the complimentary compensated solenoid, so the principle of shortest magnetic lines is satisfied. The magnetic lines through the strand are connected in the proximity at the open ends and this is the area where the tRNA molecule attaches a proper amino acid.

The proteins synthesized according to the DNA code have different sequences of amino acids and their taxonomy exhibits a large diversity. While the model of the complementary compensated solenoids is not valid for the proteins, they still could be analysed by a single solenoid model. If accepting that a unidirectional cascade state transfer is possible through the bonding path of the molecular chain, then a single solenoid model could be used for the helices of the protein. In such aspect, the analysis of the secondary and tertiary structures of the proteins leads to the following considerations:

(a) Different types of secondary structures as helices, sheets, beta turns, bulges and so on provide different structures of magnetic fields.

(a) The magnetic field from the unidirectional cascade state transfer may influence the common positions of the secondary structures

(c) The bond angular positions between neighbouring atoms are restricted by the strong conditions of finite nuclear structure and restricted angular freedom of the chemical bonds

(d) Discrete type of rotational freedom with some finite deviation is possible between single valence bonds

(e) The above mentioned considerations and spatial restrictions lead to a conclusion that an overall asymmetry of the magnetic filed from the secondary structures (mainly from the helices) may exist. Then the tertiary structure may try to restore the asymmetry of magnetic fields arisen from the diversified secondary structures by obtaining an overall symmetry at some higher structural order. Simultaneously, this will be accompanied with a tendency of shortest (as possible) magnetic lines.

(f) The cascade energy transfer through the bonding path of the protein chain might be accompanied with some ion current, whose energy could be also involved in the total energy balance.

The taxonomy of 3D protein structures is well described in the book Advances in Protein Chemistry[9] (1981) by C. B. Anfinsen, J. T. Edsall and F. M. Richards.

The stiffness of the secondary order structure is larger than the stiffness of the tertiary one. This matches the strength of the mechanism involved in the restoration of the overall field symmetry. As a result every protein may have a sustainable native shape when placed in proper environments (temperature, pH, ATP).

The provided analysis helps to explain one of the problems in molecular biology, known as a Levinthal's paradox: "Why the proteins folds reliably and quickly to their native state despite the astronomical number of the possible quantum states according to Quantum mechanics?".

Now let find out how the protein may react if the condition of shortest magnetic lines is temporally disturbed by some external factor, for example, by addition of Adenosine triphosphate (ATP). The ATP carries stored energy in its rings. When the chemical reaction $ATP + H_2O \rightarrow ADP + P$ occurs the stored energy might be induced in some rings in the protein under consideration. This may change the conditions of the compensated magnetic field (related to the principle of shortest magnetic lines). Then the reaction leading to restoration of the energy balance (involving the magnetic energy) could involve some kind of change of the shape of the protein that could invoke some motion. **This may eventually explain the protein motility in proper environments (temperature, pH, ATP concentration) that is related with a temporary change of its higher order shape.**

### 10.5.3. Environment considerations for preservation of the native shape of the proteins.

Many proteins have a complex 3D structures comprised of secondary helix and tertiary structures. They exhibit amazing tendency to preserve their 3D shape in proper environment conditions in which the temperature is one of the important factors.

The electronic bonds and hydrogen bonds allow some freedom of the 3D structure of biomolecules. It is known from the Quantum mechanics that the excitation of particular vibrational-rotational band of the molecular spectra is temperature dependant. Translated to BSM model this dependence means **activation of proper subharmonic number from the available set of the quantum orbit for each electronic bond.**

Consequently the complex 3D shape of the biomolecules is dependable of two main features:

(a) a proper subharmonic and quantum number of every bonding electron

(b) a same subharmonic and quantum number of the similar interatomic bonds along the molecular chain

The feature (a) puts a restriction for the absolute temperature range in order to preserve the native state of a long chain molecule, while the feature (b) puts a strict requirement for a temperature uniformity along the molecular chain. This, of cause is not the only factor. Additional factors are the interactions between the highly oriented atomic ring structures discussed in previous paragraphs and the conditions for H-bondings.

Another environmental conditions that are also important, for example, are such as the pH factor and ATP concentration. The first one may assure the proper ion current conditions (according consideration (f) in section 10.5.2, while the second one - the necessary energy.

### 10.5.4. Magnetic field involved in the higher order structures of DNA.

The DNA molecules of the single cell organisms are usually of circular type with a supercoiling. The DNA molecules of eukaryotes, however, are of linear type with much more base pairs and complicated secondary and third order structures.

According to the principle of the shortest magnetic lines and compensated magnetic field, the circular DNA should be more resistant, because the magnetic line paths are enclosed inside of the structure. This condition might be partly disturbed only during the transcription. The linear DNA, however, possesses some additional properties that may facilitate the process of intermolecular DNA communications, according to a hypotheses presented below.

The length to diameter ratio of DNA is very large. It is extremely large especially for eukariotic DNA. For human chromosomes, for example, the average ratio is in order of $1x10^7$. In order to be held in a tiny space of cell nucleus such long molecule have higher order structure, known as supercoiling. The mechanisms involved in the formation and sustaining of such a structure has not been completely understood so far. The following analysis put some light about the possible mechanisms.

Let presenting briefly some of the experimental observations about supercoiling features of a long DNA. In a paper[10] "DNA-Inspired Electrostatics" in Physics Today by W. M Gelbart et al. (2000), the authors provide a summary about one important feature of DNA. They say: "Under physical conditions (a 0.1 molar solution of NaCl), a DNA molecule takes on the form of a disorder coil with a radius of gyration of several micrometers; if any lengths of the molecule come within 1 nm of the other, they strongly repel. But under different conditions-in a highly diluted aqueous solution that also contain a small concentration of polyvalent cations - the same DNA molecule condenses into a tightly packed, circumferentially wound torus." Fig. 17 shows the toroidal shape of DNA from the same paper[10]. The figure has been adopted from O Lamber et al., *Proceedings of the National Academy of Sciences* (USA), vol. 97, p.7248, (2000).

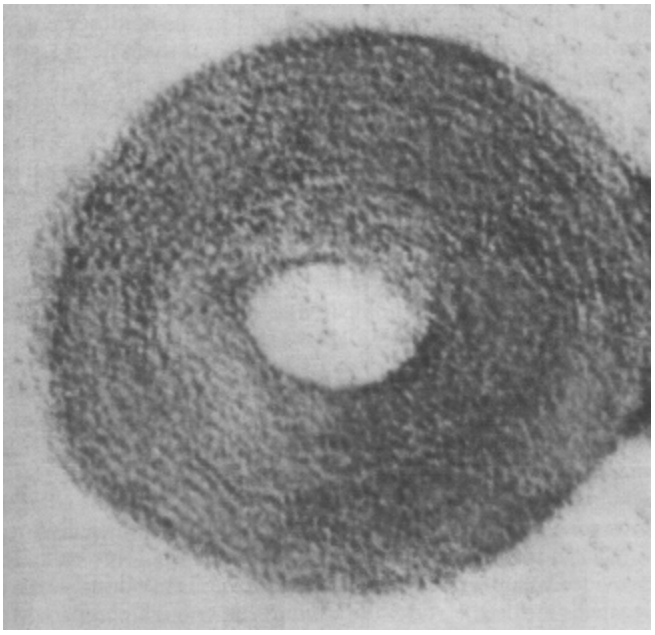

**Fig. 17** Toroidal DNA condensates, Courtesy of O. Lambert et al. *Proceedings of the National Academy of Sciences* (USA), vol. 97, p.7248, (2000).

The DNA molecule is usually negative charged, so the repels between the different part of the long chain molecule in close distance (about one nm) is understandable. However, why the DNA folds in such packed toroidal structure in a presence of proper polyvalent cations? This effect gets reasonable physical explanation by BSM theory if analysing the magnetic field conditions at a CL node level.

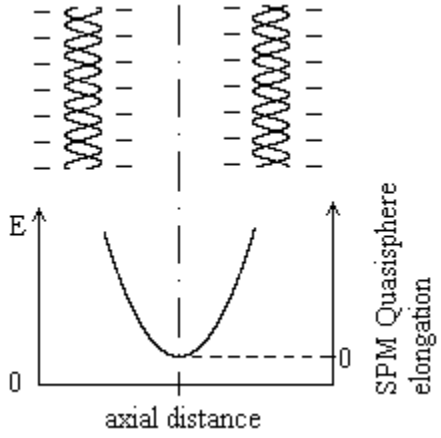


**Fig. 18.** Electrical field and SPM Quasisphere elongation between two parallel parts of DNA

Fig. 18 shows the electrical field intensity between two parallel parts of DNA. The left vertical scale axis shows the electrical field intensity, while

the right vertical axis shows the elongation of the SPM quasispheres in the plane of drawing. One specific feature is apparent from the drawing: the elongation of SPM quasispheres becomes zero in the middle between the parallel strands. (see "Brief introduction to BSM theory.."[4] or Chapter 2 of BSM for more details about the Magnetic and and Electrical quasispheres of SPM vector). This is possible only due to the strong spatial orientation of the Electrical Quasispheres (EQ), contributed to the E-field along the parallel DNA parts. Consequently, the elongation of all SPM quasispheres in the plane passing through the parallel DNA axes is reduced to zero. Then these SPM quasispheres become of Magnetic Quasisphere (MQ) type. In the same time the SPM vector of these MQs might be synchronized, because the interacting EQs from the parallel long chains could be easily synchronized. Then the obtained in such way MQs provides excellent conditions for a permanent magnetic field. In order the its direction to be stabilized, however, it needs some complementary interactions (having some inertial features) with some external current involving charge particles. Such current may be provided by some heavy and polyvalent ions (because the masses of the light ions Na and Cl are not so different and their charge is not enough large. The currents from the positive and negative ions with overall helical trajectories are expected to have different paths. This could happen if they have different masses, because they will get different centripetal acceleration in a helical trajectory. The supercoiling shape of the long DNA will provide a necessary condition for such trajectory. In the same time the condition of shorter magnetic lines will keep the supercoiled DNA in compact configuration, while the negative charge of DNA strands will keep the proper distance between the different parallel parts of the molecule.

The explanation of the DNA supercoiling in eukariotic cells in a natural cell environments requires some additional considerations. The human DNA, for example, is supercoiled around a protein called histon octamer. Presently, the shapes of the higher order structures of DNA as a nucleosome formation, a Chromatin and a Chromosome are well known. They are illustrated by Fig. 19.

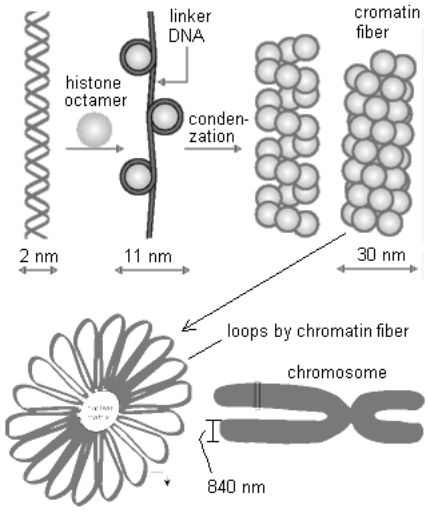


**Fig. 19.** Higher order structures of DNA in Chromatin and Chromosome

The conclusion (A) in §10.5.1 provides an explanation why the DNA molecule is easily folded as a secondary helix around the histone octamer. The latter, evidently, provides a higher order helical shape conditions. According to the considerations in §10.5.1 and §10.5.2, the histones may also have features of energy flow. If examining the atomic structures of the histones (by using the Protein data Bank) we will find that two type of atomic rings: (6C) and (N+4C) are involved into the building blocks. A possible energy flow through the spatially arranged rings may play a role in the DNA bending and coiling around the histone octamer.

The Chromatin, known as a chromatin fibber (with diameter of 30 nm) is additionally coiled into a daisy flower shape, called a chromosome miniband. The chromosome miniband, shown in the left bottom side of Fig. 17 contains 18 loops of daisy flower shape. A stack of daisy flower minibands arranged in a superhelix with diameter about 840 nm forms a chromosome.

The discussed effect of magnetic field creation with sustainable ion current might be part of the complex mechanism sustaining the supercoiled structure of the human chromosome. The balance between the magnetic field, the ion current and the electrochemical potential will depends from the internal cell environments as in the case of the proteins. Simultaneously, the principles of the shortest magnetic lines and compensated magnetic field

should also play some role. When one of the both ends of the chromosome is attached to the cell the ion current and the magnetic field will be stabilized, so the supercoiled shape will be stable. If the chromosome, however, is not attached by some reason, a small change in the ion current will cause a reaction of the magnetic field. This may invoke a shape change and a motility of the chromosome.

### 10.6. Hypothesis about a DNA involvement in a cell cycle synchronization mechanism

#### 10.6.1 General considerations

The cell cycle synchronization is an important factor for a normal organ formation in the growing multi-cellular organism. One simple example demonstrating its importance is the eye formation. Some not synchronized cell division in early phase of eye formation may lead to significant defects.But, how the enormous number of individual cell know when exactly to enter into mitosis? If assuming that an autonomous clock mechanisms in the cells are involved, they could be asynchronized after a number of cycles. A synchronization by chemical messengers passing through the bulk of enormous amount of cells is also not quite convincing for synchronized growing of organ like eye, for example, consisting of many thousands cells.

It is reasonable to expect that DNA might be involved in the cell cycle synchronization. The analysis of DNA at atomic level by BSM concept led to formulation of hypothesis about electromagnetic intercommunication capability of DNA molecules located in different cells of a same type. The proposed hypothesis relies on a pure physical mechanism some of the features of which has been discussed.

Let use the concept of complimentary compensated solenoids described in §10.5.1., but regarding the both complimentary parts of this system as separate helices. In this case, they could be considered as two solenoids serially connected in circle. Then the direction of cascade energy transfer through both strands of DNA (corresponding to the two separated solenoids) could be a clockwise or counter clockwise. This will define two different directions of the magnetic lines. Let suppose, that the obtained magnetic field is involved also in some interaction processes in the cell, so it could not be reversed spontaneously. This means that the direction of the cascade energy flow will be kept stable in respect to the helical direction. Let denote the direction of a stable energy cascade through one strand to be +z. This direction regarded as axis +z in fact is not a straight line, but a helix geometrically centred along one of the DNA strands. Obviously, the stable energy flow through this strand will influence the direction of the rotating energy states (handedness) in the attached (O+5C) rings. Thus we may accept that they all have a clockwise direction coinciding with the rotating direction of the running energy cascade through DNA strand along +z axis. In other words all stored energies in (O+5C) rings have the same handedness. Note that the definition of handedness of the rotating energy states in the rings is referenced to the direction of the cascade energy flow.

Let now pay attention about the energy storage capability of Purines and Pyrimidines involved in DNA. The pyrimidins Cytozyn (C) and Thymin (T) have single rings (2N+3C) with electronic bond connection to the DNA strands. The Purines adenine (A) and Guanine (G) both have two attached ring structures (2N+3C) and (2N+4C) that are also connected to the DNA strands. Because, the single rings of C and T are the same as the attached rings of A and G, we may accept that they carry one and a same amount of stored energy.

The Purines and Pyrimidines have stronger bond connections to their own strand, than between themselves as base pairs. The handedness of their stored energies could be also influenced directly by the handedness of the energies in the (O+5C) rings from the strands. Using the same logic, the (2N+3C) rings should get the proper handedness from the strands to which they are strongly connected. The attached to them (2N+4C) rings however will get a complimentary opposite handedness.

Now let consider the normal situation, when the both strands of DNA are closely spaced in a shape of double helix. If aligning the DNA along a new defined axis +Z, the rotated energies in the rings connected to one selected strand, say a first one, will have a clockwise rotation, while from the second one - a counter clockwise. Consequently, when introducing a common direction axis (+Z) for

both strands, the energies from (O+5C) connected to the two strands of DNA will look as they have different handedness. (In the further analysis, the common +Z axis will be considered for both strands).

Table 3 provides the handedness of the stored energies for all types of rings in DNA molecule, as a result of the above analysis. The handedness of stored energy in any kind of ring is referenced to a common axis Z+ of the DNA molecule.

Energy and handedness states Table 3

| strand A | strand B | Energy states for |
|---|---|---|
| $E_S$/\| | $E_S$\|/ | (O+5C) ring |
| ($E_1$/\|\)($E_2$\|/) | ------- ($E_1$\|/) | A---T and G---C |
| ($E_1$/\|\) | ------- ($E_2$/\|\)($E_1$\|/) | T ---A and C---G |

Notations:

/|\ and \|/ - denotes two states of handedness

ES - a rotating state energy in (O+5C) ring

E1 - a rotating state energy in (2N+4C) ring

E2 - a rotating state energy in (2N+3C) ring

----- a connection by hydrogen bond

($E_1$/|\)($E_2$\|/) - energy states with complimentary handedness in attached rings

Let examine, now, how the stored energies in the rings of different types could be influenced from some change of cascade sequence. The energies of (O+5C) rings can be easily affected by a change in the energy cascade flow through the strand, because the strand bonding path passes through C=C bond of every ring. The stored energies in single (2N+3C) rings could be affected by the change of the cascade type energy flow through (O+5C) rings. The stored energies in the attached rings (2N+3C) and (2N+4C), however, is of complimentary type, so it is more resistant to the mentioned above energy flaw changes.

Summarizing the above considerations we may conclude:

(1) The stored energy sequence in (O+5C) rings (with unit value of $E_S$) is strongly influenced by a change in the cascade energy flow through DNA strands

(2) The complementary energies ($E_1$/|\)($E_2$\|/) in the attached rings are more stable than the energy $E_1$ in the single ring.

(3) A change of energy sequence in (O+5C) rings could influence stronger the stored energies in the single (2N+3C) rings than in the (2N +4C) rings.

(4) The energies $E_1$ and $E_2$ from connected by H bonds A--T and G--C have always the same handedness.

Now, let consider that the DNA strands are opened in one end only. In such case, the paths of the magnetic lines is increased at this end. It is known from the physics that if some alternative field components appear in such conditions, some energy will be emitted as EM waves. At this point, however, we must consider some specific features of the double helix structure DNA:

The (O+4C) rings, arranged in a helix, contains equally spaced gaps. Having in mind the enormous number of these rings, the cascade energy transfer will have a very large unidirectional component but quite a small alternative component for one clock. Then it is reasonable to accept that the generated magnetic field will have the same unidirectional feature like the field from the energy cascade through the strands. This means that every emitted pulse will have energy of $2E_S$.

When considering the energies of single rings (N2+C4), however, the emission conditions are different. They do not form uninterrupted sequence along the chain as the (O+4C) rings, so the sequence of the released $E_1$ energies can not possess an own permanent component. This might affect the preferred direction of the magnetic field generation. The helicity of DNA and higher order helicity of chromatin and chromosome with some complimentary ion currents may also provide conditions of energy release from (O+4C) rings in one and a same direction for both strands. It is reasonable to accept that the emitting direction could follow the direction of emptying the energies of (O+4C) rings. Let considering that this direction corresponds to the introduced +Z axes. Fig. 20 illustrates the sequence of emptying the stored energies in (O+4C) rings (with individual energy $E_S$) and (2N+4C) rings (with energy $E_1$). The energy status and the direction of energy emission are shown for two consecutive clocks (i) and (i+1). The energies stored in the two attached rings (2N+4C) and (2N +3C) are not shown in the figure, but they are always complimentary to the (O+4C) rings.

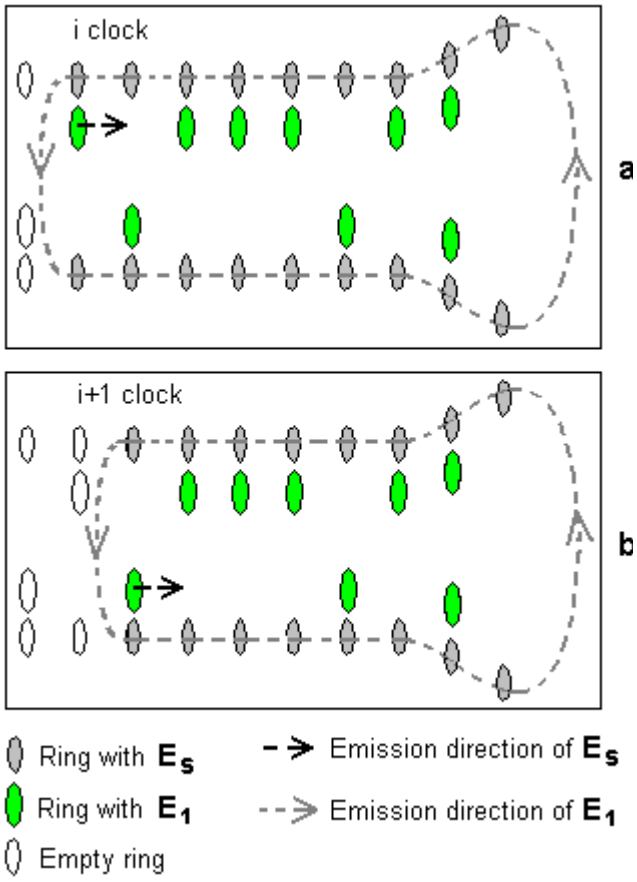


**Fig. 20** Energy status and direction of energy transfer for two consecutive clocks. The emitting direction is along +Z axis

The handedness of all $E_S$ energies in respect to the direction of the permanent magnetic field (defined by the cascade energy transfer through the bonding path) indicated by arrows in a dashed line is one and a same. When emitted by the common +Z direction the corresponding $E_S$ energies contribute to a common $2E_S$ pulses. For $E_1$ energies, however, the emission conditions are different because they do not have a stable unidirectional sequence. Then considering the energy emptying direction +Z the handedness from $E_1$ belonging to the different strands are different (clockwise or counterclockwise in respect to +Z axis). Let considering:

(a) The $E_1$ energies with clockwise handedness in respect to +Z axis provide a photon sequence with a clockwise phase difference between the photons.

(b) The $E_1$ energies with a counter clockwise handedness in respect to +Z axis provide a photon sequence with a counterclockwise phase difference between the photons.

(c) The emitted photons of $E_1$ energies from the same strand are entangled with preserved phase difference. The phase advance in one strand (with +Z orientation of its cascade energy) will have a clockwise phase sequence, while from the other strand it will have a counter clockwise.

(d) Anyone of the both sequences of entangled photons contains embedded information about the A--T and G--C sequence of DNA referenced to one strand.

(e) The energy of entangled photon sequence is less dispersive in conditions of intercellular transmission.

(f) The probability of absorption of the entangled photons is much higher if meeting a similar spatially arranged atomic rings.

(g) If the process of DNA energy release is invoked not by internal factor, but from externally induced synchronization, it might have some phase delay, due to a missing of the initial synchronization sequence.

The photon entanglement, as a physical phenomena) is observed in lasers. Firstly, two entangled photons have been observed few years ago. Observation of three entangled photons has been published by Zelinger group[11,12] (D. Bouwmeester et al, 1999). The authors express opinion for “entanglement between many more particles”. The same group later reported observation of four entangled photons and provided also experiment of stimulated emission of polarized-entangled photons[12] (A. Lamas_Linares, J. C. Howell & D. Bouwmeester, 2001). In the conclusions of latter article they write:” We consider that entaglement robustness-together with the rotational symmetry of the state created by stimulated polarization entanglement - opens the way to many applications in quantum information, and provides a powerful tool for studying the almost unexplored area between the discrete and the macroscopic optical quantum correlation experiments.”

Experiments with entangled photons show that the entangled states fight the diffraction limit valid for a single photon. This may provide explanation of the mentioned above feature (e).

It is reasonable to consider that conditions of uniform temperature and proper spatial arrangement of the ring structures in DNA may provide the possibility for multiple photon entanglements in the described above mechanism. It is known from the single mode narrow line emitting lasers that their coherence time is quite long. Let for example accept that the coherence time in the DNA emitting process is in order of 1E-12 sec. If an average lifetime for a single bond is about 1E-14 sec, then the time between two $E_S$ clocks is 6E-14 sec (six bonds). In this case, the entangled sequence will include a binary code corresponding to 600 $E_S$ clocks. Such binary code corresponds to 600 bp (base pairs) and involves 200 codons.

Now let pay attention about one particular problem related to DNA investigation, known as a **C value paradox**.

**A substantial fraction of the genomes of many eukariotes is comprised of repetitive DNA in which short sequences are tandemly repeated in small to huge arrays.**

Tandemly repetitive sequences, known as "satellite" DNA's are classified into three major groups;

-satellites - with repetitive lengths from one to several thousands base pairs.

- minisatellites - repetitive arrays of 9 to 100 bp, but usually 15 bp, generally involved in mean arrays lengths of 0.5 to 30 kb.

- microsatellites - repetitive arrays of short 2 to 6 bp found in vertebrate, insect and plant genomes.

The code of repetitive sequence does not encode amino acids. The percentage of this non-informative DNA increases significantly with organism complexity but depends also of other factors. Among them are the living environment conditions of the species.

From a point of view of proposed hypothesis, the C value paradox obtains quite logical explanation:

**(h) The repetitive sequences in DNA code provide repetitive synchronization code that may increase reliability of the DNA intercellular communication.**

A large number of not discussed here diversified features of the DNA redundancy in different organisms and species could find a logical explanation from the point of view of feature (h).

For example, the shown below repetitive sequence in DNA from Drosophilia corresponds to the following binary codes embedded in two entangled photons, related to the two strands:

(AATAT)n, where n - is number of repeats
from DNA strand 1: (00101)n
from DNA strand 2: (11010)n

If the emitted entangled photon from strand 1 contains CW circular phase sequence of the code, the emitted entangled photon from strand 2 will contain CCW circular phase sequence of the complimentary code.

It is evident that the entangled photons carry embedded code that is dependable of both: the amino acid code and the redundancy code. This dependence may eventually play a role in the immunological response to transplanted tissues or organs. The redundancy code greatly increases the probability of successful synchronization. Then it is reasonable to expect a large abundance of repeatable code near the end side of the linear DNA in eukariotic cells that is an observed fact.

### 10.6.2. Time sequence in the energy read-out process of DNA and its possible relation to the cell cycle synchronization.

Let consider some initial state of DNA molecule when all rings are charged with their normal energies $E_S$, $E_1$ and $E_2$. In some moment invoked by internal or external triggering, the stored energies start to clock out with synchronization sequence $E_S$ and two entangled photon sequences. Ones this process is started it will be self sustained until all $E_S$ energies states are read-out. We may call this effect a read-out process of DNA. The time duration ($t_{total}$) for DNA read-out should be

$$t_{total} \approx 6 t_{av} \frac{DNA \text{ length}}{0.34 \text{ nm}} \qquad (10)$$

where: $t_{av}$ - is the average lifetime of excited states in the bonding path of DNA strand, 0.34 nm is the distance between the rings of the neighbouring base pairs.

The total read-out time is very short. For DNA with length of 1 *m* and $t_{av}$ ~ 1E-14 s the read-out time is only 0.18 ms.

After the DNA is read-out, all $E_S$ energies are emitted. The $E_1$ energies only of the T and C are emitted, but the complementary state energies $E_1$ and $E_2$ of A and G are preserved due to the attached rings. This invokes some type of asymmetry between connected Purines and Pyrimidines by H-bonds. Such conditions may help for separation of the DNA strands for initiating of the replication process.

Now, let analyse the possible involvement of DNA read-out process in the cell cycle synchronization in eukariotes. We will not discuss here the complex processes of cell cycle regulation in which the proteins are involved, but only the conditions of successful triggering and read-out of DNA. We may assume only that every individual cell possesses some kind of local triggering mechanism. Such mechanism is necessary but not enough condition in order to initiate the read-out process. The DNA read-out can be successful only if conditions for emission of EM energy exist. Consequently it will depend of the following conditional states of DNA molecule:

(a) The two strands of one end of DNA must be separated (or unbalanced by promoter) in order the EM quanta (photons) to be emitted)

(b) The two strands (not counting the end conditions mentioned in (a)) must be completely symmetrical in order the read-out process to be self-sustainable.

The requirements (a) and (b) excludes the mRNA attachment to DNA or any other regulatory protein, so the transcription process and regulatory mechanisms should be completed. Then the optimum conditions for development of synchronized read-out as an avalanche process should be the phase S (start of DNA replication).

Now let assuming that the internal triggering mechanism provides triggering clocks with period much shorter than the cell cycle. They will not provide successful triggering until the conditions (a) and (b) are satisfied. However, once they are satisfied the DNA read-out will be successful. Then the emitted entangled photons with a large common energy and encoded sequence possess an increased probability for activation of similar read-out processes in the DNA of the neighbouring cells. The extremely fast read-out process could lead to similar read-out process in many DNA. In such case, the emitted entangled photons may additionally interfere and contribute to the avalanche process of the synchronization. The avalanche process, however, will be contributed only of DNA molecules that do not have significant differences. In case of tissue and organ transplantation, the avalanche process will not work between the DNA from different species whose synchronization sequences are too different and even the not decoding pieces (related to the C value paradox) might play an important role.

### 10.6.3. Environment considerations for the efficiency of the avalanche process

The phase accuracy of the cell cycle synchronization evidently depends of the individual cell cycle phases and environmental conditions.

#### 10.6.3.1 Phase accuracy dependence of the cell cycle period

If considering the triggering of the synchronization from internal cell mechanism in a proper phase of the cell cycle, the period between two consecutive synchronization bursts will depend of the time lag between the local clock triggering events. Evidently the period of these events should be much smaller than the cell cycle period.

Let accept that the individual cell cycle regulation mechanisms provides a Gaussian type distribution of the cell cycle period from many cells. Then the optimum conditions for avalanche read-out should be expected in some moment that is closed but not overpassing the maximum of the Gaussian curve. **Once it is initiated, the Gaussian curve will be cut down for all cell contributing to the avalanche.** Those who had performed a preliminary read-out and those not activated by the synchronization will not contribute. The cells in which the transcription and regulation processes are not completed in this moment will also be excluded and their mitosis will not be in harmony with the synchronized cells.

Additionally we may not expect that all the synchronized cells will be activated in the very beginning of the read-out of the first activated cells. The repeatable sequences may provide conditions for larger number of entangled photons. Such photons posses also an increased probability for absorption and activation of similar repeats from

DNA in other cells. **Consequently the tandemly repetitive sequences of DNA increase the probability for avalanche development of DNA read-out.**

### 10.6.3.2 Physical factors of cell environment

The most important environmental factor for successful EM synchronization is the temperature.

It is reasonable to assume that the cascade energy transfer through the bonding path of the DNA strand is phase synchronized by the energy rotation cycle in the (O+5C) rings. The duration of this cycle is:

$$T_R = t_O + 5t_C \quad (11)$$

where: $t_0$ and $t_c$ are respectively the lifetimes of the excited states in oxygen and carbon

The period, $T_S$, of the synchronization pulses is defined by the sum of the consecutive lifetimes through the bonding path of the strand, shown in Fig. 13

$$T_S = t_C + 5t_{av} \quad (12)$$

where: $t_{av}$ is the averaged lifetime value of the bonding electrons involved in the bonding path of the strand.

Then the condition for mentioned above phase synchronization is expressed by the relation:

$$T_S - T_R = t_0 - 4t_C - 5t_{av} = const \quad (13)$$

The expression (13) is a constant for all involved DNA molecules if the same energy levels of the excited states are involved. This is a quantum mechanical condition that will depend only of the temperature. The successful generation of entangled photons, however, is additionally dependent of the correct spatial arrangement of the (2N+4C) rings. If the DNA molecule is sharply bent or it is in proximity to a protein involving magnetic field asymmetry, the necessary conditions for generation of multiple photon entanglement will be disturbed. This will affect the efficiency of the synchronization process. Formations of Cruciforms, for example, may affect the emitted sequence. Z-type DNA inclusions and any external influences causing a helical non-uniformity of Beta type DNA may also block the successful read-out process.

**The synchronization is possible in limited temperature range and good temperature uniformity along the DNA chain. The synchronization efficiency is dependent of the bending conditions of DNA and the spatial and helical uniformity along its chain. External factors causing any modification of the spatial parameters of the DNA double helix may inhibit or disturb the readout process.**

## 10.7. Established features and experimental results supporting the hypothesis of the DNA involvement in the cell cycle synchronization

Many properties of the DNA molecules in eukariotes are in good agreement with the features of DNA according to the provided analysis.

### 10.7.1 Absorption properties of DNA.

DNA absorbs ultraviolet light in the range of 240 to 280 nm with a maximum at about 260 nm. Increasing the temperature destabilizes the double helix. Experimental observation leads to a conclusion that the thermal stability of DNA is a function of base stacking, and not only of the hydrogen bonding[13] (Saenger, 1984). This is in agreement with the suggested mechanism of stabilizing magnetic field due to the cascade energy flow through the bonding paths of the DNA strands.

The mechanism of energy store and release suggested by the presented hypothesis is in agreement with the observations, reported by Joseph Lakowiccz et al. (2001) in a paper[14] “Intrinsic Fluorescence from DNA can Be Enhanced by Metallic Particles”. They use silver particles of size about 4 nm put in the surface of two quartz plates with distance between them of 1 - 1.5 um. The DNA placed in this gap has been excited at 287 nm by pulse sequences from a dye laser with a 100 ps pulse with. The intrinsic emission following such excitation in the range from about 330 to 350 nm is increased about 80 times around the metal particles. The detected radiation they believed to be from adenine and guanine.

The authors explain the effect by a decreased lifetime in relation with the SERS effect (Surface-enhanced Ramman spectroscopy). Nevertheless, they also acknowledge the existence of another less understood effect. The obtained results of time dependent intensity decay are shown in Fig. 21 (corresponding to Fig 5 of their publication).

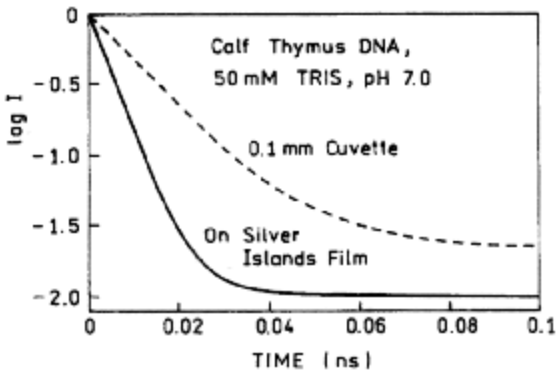


**Fig. 21** Time-dependent intensity decay of DNA without metal (-) and between silver island film (Adapted from J. R. Lakowicz et al., 2001).

The explanation of the observed effect from a point of view of BSM theory and suggested hypothesis is a following. The laser pulse charges the energy storage rings of DNA. The silver metal islands introduce not uniformity field conditions in the proximity of DNA. In such conditions, the mechanism that may keep the stored energy in the rings is disturbed. As a result, in the DNA portions that are in close proximity to the metal islands a spontaneous read-out process may occur sporadically. This will appear in a shorter time interval between the excited pulse and the fluorescence emission in comparison to the case when DNA is not in proximity with such particles. This corresponds to the observed decreased lifetime. It is interesting to note that the fluorescence lifetime is still much longer than the lifetime in a single electronic bond. This means that the stored energies in the rings may exist not for one but but for number of rotational cycles.

### 10.7.2 Increased binding ability of some simple organic molecules

The proteins that bind to DNA are usually very large molecules containing thousands of atoms. But some comparatively simple organic molecules also have an increased ability for binding. When examining such molecules we see that they posses attached atomic rings. As was mentioned before, the energy in such rings is more stable. This gives them additional ability to interact with DNA due to magnetic field interactions. Such molecules for example are:

Trimethylpsoralen: 3 attached rings
Ethidium Bromide: 3 attached rings + 1 single
Chloroquine: 2 attached rings.

### 10.7.3 Effects of the salt concentration in helical winding and DNA supercoiling

As the concentration of a monovalent cation ($Na^{+}$) or divalent cation ($Mg^{+2}$) increases to high levels, the DNA double helix becomes wound less tightly.

According to the suggested hypothesis, the ion concentration influences the ion currents involved in the stabilisation of the magnetic field of DNA, responsible for its supercoiling shape.

### 10.7.4 Role of the intermolecular triplexes in the genetic recombination

Regions of triplex DNA formations have been identified near sites involved in genetic recombinations. They usually have a mirror symmetry repeats of base pairs (as AGGAG). Kohwi and Panchenko[15] (1993) found that the formation of intramolecular triplex structures in DNA in vivo can induce genetic recombination between two direct repeats flanking the triplex formed sequence.

According to the proposed hypothesis, the triplex formation in DNA disturbs the symmetry of the compensated field solenoid of DNA. Instead of flowing in the internal region of DNA double helix, some of the magnetic lines are forced to pass through the external region. In conditions of chromosome recombination in vivo, the read-out process may be more often, than in the regulated cell cycle. Then the emitted sequence of entangled photons from one chromosome could be directly induced into the other. This may influence their common position and orientation. In the same time the magnetic field of the cascade energy transfer through the bonding path of the DNA strand is not compensated in the triplex region. When combining with a similar region from another chromosome the complex magnetic field may become compensated and stable.

### 10.7.5. Electronic properties of DNA

This subject is of increased interest of physicists and chemists. Despite the subject is far from new, it is very controversial. A recent overview pa-

per about this topic is presented by C. Dekker[16] in Physics World, 2001. The experimental results deviate from good insulator to good conductor, while many researchers consider that DNA is able to provide some kind of energy flow.

Currently, two possible mechanisms of charge transfer are accepted: a coherent process of single step electron tunnelling and a thermal hoping. It is interesting that a signature of cascade transfer exists in both suggested processes. While this theoretically suggested mechanisms seam reasonable, direct electrical measurements by number of physics groups provide conflicting results. The results reported by Hans-Werner Fink and Christian Schonenberger (1999), for 1 $\mu m$ long DNA in vacuum indicate a good conductivity[17]. However, this contradicts to the accepted theoretical considerations where DNA is expected to behave as a semiconductor with a large energy gap between the valence and conduction bands. The experiments of Porath and co-workers (2000), for example, on a particular type of DNA - called poly(gG)-poly(dC) DNA and show that it behaves as a large gap semiconductor[18].

One important fact that may influence the experimental results is the different environmental conditions at which the experiments are performed. Additionally, in number of experiments the electronic properties are not directly measured, but derivable from the transient absorption spectra.

Let try to explain the possible electrical properties of DNA from the point of view of BSM models. In order to have a stable energy cascade transfer, the DNA must be in proper environments (pH, temperature, ATP) and to be enough long. In normal environments, it is considered a negatively charged. This charge, however, is uniformly distributed, so it may not influence the energy cascade transfer. In such case, the stored ring energies are synchronized and have a proper handedness. For small voltage along DNA, the electrons do not quit their spatially distributed orbits. For large voltages, however, the proximity proton field defining their orbits are biased, end the valence electron could jump synchronously. This transition, however, is expected to interact with the rotating energy states in the rings. The signature of such interaction might be the effect of “single step electron-tunnelling mechanism”. It is evident that such conditions may occur only if a stable energy cascade transfer through the DNA strand exist, but the latter effect is possible only at proper environments.

## 11. Hypothesis of decoding process in some of the complexes aminoacyle-tRNA synthetases - tRNA.

### 11.1. General considerations and code analysis

The prototype of tRNA molecule is coded in the gene. The current estimate for number of tRNA in animals and plants is up to 50. The typical shape of the tRNA is shown in Fig. 16. The tRNA binds to the proper enzyme that charges to its end one of the 20 amino acids corresponding to the anticodon. Aminoacyl-tRNA Synthetase is a family of 20 enzymes whose structures are pretty well known. The enzymes usually recognize the corresponding tRNA using the anticodon.

Let analyse the coding of the amino acids based on the anticodons used by tRNA. Instead of anticodons we may use for convenience the most popular RNA codons, given by Table 12.1 (in a general case the anticodon code is directly obtainable from the corresponding codon code). Their number is 64. One exclusion from that rule is the anticodon of Alanine, where the three codes GCU, GCC and GCA are presented by one codon CGI ( I - Ionosine). This reduces the total number of anticodons to 61.

One of the features of the amino acid coding, that is evident from the table, is the **code redundancy**. Most of the amino acids are coded by more than one codon. One additional surprise comes from the genome analysis. Some organisms don’t have genes for all twenty aminoacyl-tRNA synthetases, but they still use all twenty amino acids to build their proteins.

The synthetase mechanism of the Aminoacyl-tRNA synthetases involves two steps. In the first step they form an aminoacyl-adenylate in which the carboxyl of the amino acid is linked to the alpha-phosphate of ATP by displacing pyrophosphate. In the second step, if only a correct tRNA is bound, the aminoacyl group of the aminoacyle-adenylate is transferred to 2’ or 3’ terminal OH of the tRNA.

**Table 12. 1**

| | | | | | | | |
|---|---|---|---|---|---|---|---|
| UUU | Phenylalanine | UCU | Serine | UAU | Tyrosine | UGU | Cysteine |
| UUC | | UCC | | UAC | | UGC | |
| UUA | | UCA | | UAA | Stop | UGA | Stop |
| UUG | Leucine | UCG | | UAG | Stop | UGG | Tryptophan |
| CUU | | CCU | | CAU | Histidine | CGU | Arginine |
| CUC | Leucine | CCC | Proline | CAC | | CGC | |
| CUA | | CCA | | CAA | Glutamine | CGA | |
| CUG | | CCG | | CAG | | CGG | |
| AUU | Isoleucine | ACU | | AAU | | AGU | |
| AUC | | ACC | Threonine | AAC | Asparagine | AGC | Serine |
| AUA | | ACA | | AAA | | AGA | |
| AUG | Start; Methionine | ACG | | AAG | Lysine | AGG | Arginine |
| GUU | | GCU | | GAU | Aspartic | GGU | |
| GUC | Valine | GCC | Alanine | GAC | acid | GGC | Glycine |
| GUA | | GCA | | GAA | Glutamic | GGA | |
| GUG | | GCG | | GAG | acid | GGG | |

The second step is conditional. This means that if a wrong enzyme is bound to tRNA the output will be zero (not charging the proper amino acids). If assuming that the process of binding the correct complex of enzyme - tRNA is occasional, then the number of possible combination for all 20 amino acid codes is $2^{20} = 1048576$. This means such number of produced tRNA and enzymes, so it is unreasonable. Another possible option is the enzymes to recognize or at least to increase the probability for binding to the correct tRNA in which case the above number could be significantly reduced.

One of the currently discussed problems is how these enzymes (aminoacyle-tRNA synthetases) recognize 20 different flavours. It is estimated that they admit intrinsically small number of errors - about 1 in 10,000. The unmistakeably recognition of 20 different flavours looks as quite intelligent task for a biomolecular structure of only few thousands atoms.

The above task could not be resolved unless the enzymes have some sensors for preliminary detection before binding and some memory. Having in mind that the enzyme contains only a few thousands atoms it is apparent that such capability should be built very economically using some basic physical properties at atomic and molecular levels. Then the sensing should be based on some simplified detection mechanism of energy states, while the memory should be based on basic physical states of binary type. Let concentrate firstly on the memory feature. The possible binary physical states for a molecule of complexity of the enzymes are following:

(1) Quantum mechanical spin of the electron

(2) direction of magnetic field (S-N or N-S)

(3) handedness of rotating energy states (according to BSM)

(4) electrical charge ( + and -)

The option (4) could be excluded because its realization requires complex structure of semiconductor type. The most reasonable option is (3) with some combination of options (1) and (2).

Let evaluate the required memory for decoding the codon of any amino acid using the Boolean algebra without minimization. Any codon is a three-digit code. Anyone of these digits needs 4 states in order to present one of the four letters (A,B,C,D). Then the three-digit code of the codon could be presented of 12 bit binary code. This corresponds to a memory map of 4096 bits. Such memory hardly be achieved by any enzyme whose molecule usually includes a few thousands atoms. Additionally the enzyme must have remote sensors for recognition of tRNA before binding and tools for test of the anticodon.

Obviously, the above general approach for decoding of 20 flavours is not feasible. We must look for some economic natural code hidden in the

codons and particularly behind their redundancy. Let analyse the redundancy using some of the unveiled properties of the ring structures and the possibility for detection of their type. The Purines are distinguishable from the Pyrimidines by the number of rings (able to carry different stored energies), so they could be sensed by some kind of binary test. The possible mechanism of such test will be discussed later. In order to see, how such consecutive tests of the first, second and third letter of the codon will lead to some results, we make the following substitution for the codons in Table 12.1.

Purines (A and G) -> 2

Pyrimidines (C and U) -> 1

The digits 1 and 2 in this substitution in fact correspond to the number of the atomic rings.

**Table 12.2**

| | | | |
|---|---|---|---|
| 111<br>111 | 111<br>111 | 121<br>121 | 121<br>121 |
| 112<br>112 | 112<br>112 | 122<br>122 | 122<br>122 |
| 111<br>111<br>112<br>112 | 111<br>111<br>112<br>112 | 121<br>121<br>122<br>122 | 121<br>121<br>122<br>122 |
| 211<br>211<br>212<br>212 | 211<br>211<br>212<br>212 | 221<br>221<br>222<br>222 | 221<br>221<br>222<br>222 |
| 211<br>211<br>212<br>212 | 211<br>211<br>212<br>212 | 221<br>221<br>222<br>222 | 221<br>221<br>222<br>222 |

Table 12.2 shows the obtained codes after this substitution. This table does not contain the names of the amino acids, but they are identifiable by the code positions. When examining the Table 12.2 we see that the binary codes (with base states "1" and "2") are in very strict order.

Let find out how many aminoacids every code from the Table 12.2 is related to. The result is shown in Table 12.3. It is evident that the distribution of the amino acid codes based on the distinguishing features between the Purines and Pyrimidines is pretty uniform. Only the codes for start and stop deviate from the uniformity of the distribution. From this simple analysis, however, one useful conclusion could be made:

**The number of possible combinations could be significantly reduced if initial binary detection of Purines or Pyrimidines is performed.**

**Table 12.3**

| Code from Table 12.2 | No of coded amino acids | Additional coding |
|---|---|---|
| 111 | 4 | |
| 112 | 4 | |
| 121 | 4 | |
| 122 | 3 | stop |
| 211 | 4 | |
| 212 | 5 | start |
| 221 | 4 | |
| 222 | 4 | |

The Purines and Pyrimidines are distinguishable by the number of rings. It will be described later that their possible remote detection have some similarity with the process of DNA readout described in section 11.6.

*a = 1* **Table 12.4**

| | | | |
|---|---|---|---|
| 111<br>111 | 111<br>111 | 121<br>121 | 121<br>121 |
| 112<br>112 | 112<br>112 | 122<br>122 | 122<br>122 |
| 111<br>111<br>112<br>112 | 111<br>111<br>112<br>112 | 121<br>121<br>122<br>122 | 121<br>121<br>122<br>122 |
| 211<br>211<br>212<br>212 | 211<br>211<br>212<br>212 | 221<br>221<br>222<br>222 | 221<br>221<br>222<br>222 |
| 211<br>211<br>212<br>212 | 211<br>211<br>212<br>212 | 221<br>221<br>222<br>222 | 221<br>221<br>222<br>222 |

Let denote the tRNA anticodon by the triplet *abc*, but using instead the corresponding codons of RNA. The following example shows the reduction of the possible combinations in three consecutive binary tests (Purines or Pyrimidines) applied for the codes of Table 12.2. Let the first test for ***a*** gives value: ***a*** = 1. This means that all codons starting with 2 are excluded from the following tests, while those starting with 1 are enabled. Only 32 from of all 64 combinations are left. This is illustrated in Table 12.4., where the excluded combinations are masked by a grey colour.

Let apply the same test for ***b*** and the result for example is *b = 2*. The available combinations are additionally reduced in half as shown in Table 12.5.

*b = 2* **Table 12.5**

| | | | |
|---|---|---|---|
| 111<br>111<br>112<br>112 | 111<br>111<br>112<br>112 | 121<br>121<br>122<br>122 | 121<br>121<br>122<br>122 |
| 111<br>111<br>112<br>112 | 111<br>111<br>112<br>112 | 121<br>121<br>122<br>122 | 121<br>121<br>122<br>122 |
| 211<br>211<br>212<br>212 | 211<br>211<br>212<br>212 | 221<br>221<br>222<br>222 | 221<br>221<br>222<br>222 |
| 211<br>211<br>212<br>212 | 211<br>211<br>212<br>212 | 221<br>221<br>222<br>222 | 221<br>221<br>222<br>222 |

In a similar way the third test of ***c***, for example, with a result ***c*** = *2* will lead to reduction of the available combinations to 8 as shown in Table 12.6.

*c = 2* **Table 12.6**

| | | | |
|---|---|---|---|
| 111<br>111<br>112<br>112 | 111<br>111<br>112<br>112 | 121<br>121<br>122<br>122 | 121<br>121<br>122<br>122 |
| 111<br>111<br>112<br>112 | 111<br>111<br>112<br>112 | 121<br>121<br>122<br>122 | 121<br>121<br>122<br>122 |
| 211<br>211<br>212<br>212 | 211<br>211<br>212<br>212 | 221<br>221<br>222<br>222 | 221<br>221<br>222<br>222 |
| 211<br>211<br>212<br>212 | 211<br>211<br>212<br>212 | 221<br>221<br>222<br>222 | 221<br>221<br>222<br>222 |

We see that by three consecutive tests the available combinations are reduced from 64 to 8, while they address only 4 amino acids. If assuming that this test is performed prior to binding of the enzyme to the tRNA, then the required combinations for a probable correct match are only $2^4 = 16$. Consequently a possible remote sensing will reduce the amount of the necessary number of enzymes and tRNA by a factor of 65536.

The additional tests for identification of the correct amino acids require distinguishing of Adenine from Uracile and Guanine from Cytozine for every letter of the triplet *abc*. The detection for such identification, however, could not be remote and perhaps is performed in the second step of the synthetase mechanism. It is known, for example, that in glutaminyl-tRNA synthetase with its tRNA the enzyme firmly grips the anticodon, spreading the three bases widely apart. Let assuming that the enzyme keeps in its memory the binary results of the previous remote detection (Purines or Pyrimidines) for every letter. Then the following test after the enzyme has grabbed the anticodon (for every letter of the codon) must be also a binary test of a type: [Adenine (A) or Guanine (G)] and [Cytozine (C) or Uracile (U)]. How could they be distinguished, while having the same number of rings? When examining their structure we see that the larger ring of Adenine includes three bonds of sin-

gle valence, while the larger ring of Guanine includes four bonds of single valence. The ring of Cytosine includes two bonds of second valence, while the ring of Uracile includes one bond of second valence. These differences of the ring structures may cause significant differences in their spectral emission-absorption properties. The very narrow temperature range will define a pretty narrow range of the population of the excited states. This may simplify the task for recognizing the differences between (A and G) and (C and U) by their spectral signatures.

After all these binary tests are performed, it seems that the correct amino acid should be decoded. However, we must not forget that the letters *abc* must be read in a correct order (from the most to the less significant digit). If this rule is not observed, the following code pairs could not be distinguished:

| | | |
|---|---|---|
| UUA | - | AUU |
| UUC | - | CUU |
| UUG | - | GUU |
| UCC | - | CCU |
| CCA | - | ACC |
| AAG | - | GAA |
| UGG | - | GGU |

Assuming that the memory map of the enzyme is naturally minimized, the correct code readout obviously must be initially detected prior to the remote sensing described above. In order to find out the possible detection mechanism for the correct code readout direction, we may examine the structure of tRNA that has been already shown in Fig. 16. In the left side of the figure, the real shape of the backbone structure is shown. In the right side of the same figure, the tRNA is presented like a flat curve in order to show more clearly some of its structural features such as, the folding of the single strand in cloverleaf shape, the position of loops, the H-bonds, the position of the anticodon and the asymmetrical ends.

The tRNA strand is similar as the DNA strand and contains regularly attached (O+4C) rings. In proper environment the tRNA could be energized, so a cascade energy transfer may occur through its strand in a similar way as in the DNA and proteins. The asymmetrically terminated end of tRNA may assure the proper direction of the cascade energy transfer. If such process is stable enough for a short time, the rotating energies in (O+4C) rings can be synchronized, obtaining in such way a proper handedness. The same is valid for the H-bonding base pairs and consequently for the codon loop. While the tRNA is not so long (75 - 90 nucleotides) the energy cascade process could not be so stable like in the DNA and the proteins. The disruption of the energy cascade will lead to synchronized readout of the rotating energy states in (O+4C) rings that could be emitted as a coherent sequence of photon pulse whose parameters (phase sequence) will carry the direction of codon readout. This readout of (O+4C) energies from its side might provoke a readout process from the base pairs in a similar way as in the DNA. The conditions for emission from tRNA, however, are different from those of DNA due to the different shape of the tRNA molecule. Let assuming a hypothetical axis (not exactly linear), defined by the twisting shape (known as a secondary structure) of tRNA and passing from the anticodon loop of tRNA to its terminating ends. The two major side loops of tRNA could be regarded as approximately symmetrical pairs in respect to the introduced axis. The supercoiling and tertiary structure may also influence the symmetry of the mentioned pairs, but will not influence the symmetrical features of the anticodon loop. In the same time, all the loops are free of H-bonds. If regarding the emission process as EM filed, it is evident that the two side loops are complimentary and will have a comparatively smaller EM emission capability (because the magnetic lines appears closed in a circle around the introduced tRNA axis). **The anticodon loop, however, does not have complimentary symmetry with another loop, so its emission capability could be much larger.** Then the emitted photons from the anticodon loop could be detected remotely by the correct enzyme. The burst of photon sequence from (O+4C) rings readout may serve as a synchronization that prepares the enzyme for detection of the anticodon. In such process the detection could be of synchronized type, so it could allow an increased probability for detection of the anticodon sequence. The tRNA could be re-energize and the readout sequence could be performed a few times. In such way, the anticodon could be detected by number of corresponding enzymes.

The remotely detected sequence from anticodon loop (carrying information for Purines or Pyrimidines) could be regarded as very fast consecutive tests of the letters in the triplet ***abc*** prior to binding of the correct enzyme to tRNA. The test results, however, will be additionally needed for the consecutive tests (A or G and C or U) that will be performed after the binding of the enzyme to the tRNA. Let assuming that these test results are directly passed to some kind of binary decoder implemented in the enzyme. Then after this remote test the number of codons from 64 is reduced to 8, corresponding to 4 amino acids. This significantly increases the probability of correct binding between tRNA and the corresponding enzyme.

### 11.2 Decoding algorithm

Fig. 22 presents the decoding algorithm according to the analysis and considerations discussed in the previous paragraph.

The remote sensing includes tests 1, 2, 3, (shown in the figure) while the other tests are performed after the tRNA is bound to the correct enzyme. The numbers in circle show the enabled codon combinations after each test. Not all the decoding tree for all 20 aminoacides is shown, but the suggested possible algorithm for their decoding is the same. It is evident, that maximum of 6 tests are necessary for decoding of anyone of the aminoacids, but some of them are decoded even at test No 5. (Leucine, for example). Two of the stop codons are also decoded at test No. 5. This provides the opportunity to use the test No. 6 for additional true test, that should increase the decoding reliability. The other stop codon UGA, however is decoded after the test No. 6. Then it could be interesting to study the statistics of UAA and UAG stop codons in comparison with the UGA stop codon (in both the RNA and DNA sequences).

According to the suggested algorithm, the tests from the remote sensing increase the probability for correct binding between tRNA and the proper enzyme, but does not exclude completely wrong bindings. It is logical to expect that only a correct binding will lead to attachment of amino acid after the tests 3, 4 and 5. The wrong binding will provide a zero result.

**Discussion.**

The first version of the theoretical analysis of the biomolecules with suggested three hypotheses[19] has been archived in the National Library of Canada in 2002. The reader of this article who has not been acquainted with the BSM theory may put one reasonable question: Why the suggested atomic models, pretending to match the physical reality, are not widely discussed and promoted by the physical society? The answer is: The alternative concept of the vacuum space is a fundamental change in physics that may affect a number of highly abstracted and mathematically sophisticated theories. This may cause a process of adaptation that could probably take years. In the fields of structural chemistry, organic molecules and nanotechnology, however, the suggested models of the atoms, could be tested and applied right away because the criterion for their validation comes simultaneously with their applications. The large data base of organic and biomolecules with known structure and atomic composition provides an excellent opportunity for reliable test and validation.

The Quantum mechanical models of the atoms are very useful for their ability to provide accurate calculation of the energy levels and interaction probabilities. The models, suggested by BSM thesis, do not intend to replace or undermine the useful features of the quantum mechanical models but to enrich the knowledge about the physical structures of the atoms and the quantum processes at subatomic level.

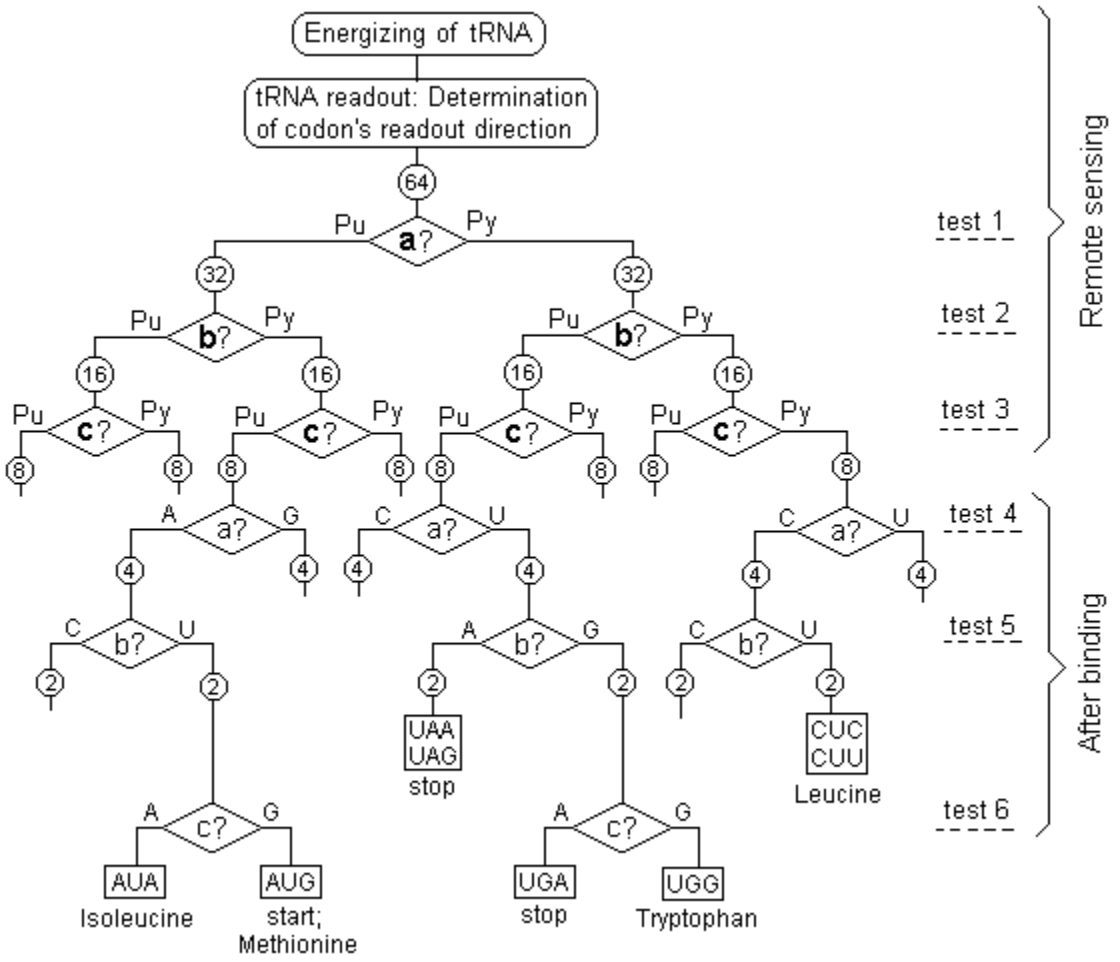


Fig. 22. Decoding algorithm according to the hypothesis of decoding process in some of the complexes tRNA - enzyme.

## References:


1. S. Sarg, *Basic Structures of Matter*, monograph, (2001),
http://www.helical-structures.org
also in:
http://collection.nlc-bnc.ca/amicus/index-e.html
(AMICUS No. 27105955)

2. T. H. Boyer, The Classical Vacuum, Scientific American, Aug. 1985, p. 70-78.

3. H. E. Puthoff, Can the Vacuum be Engineered for Spaceflight applications, NASA Breakthrough Propulsion Physics, conference at Lewis Res. Center, 1977

4. S. Sarg, Brief introduction to Basic Structures of Matter theory and derived atomic models, Journal of Theoretics, 2003 www.journaloftheoretics.com/Links/Papers/Sarg.pdf

5. H. E. Puthoff, Gravity as a zero-point-fluctuation force, Physical review A, v. 39, No 5, 1989, p. 2333-2342.

6. S. Sarg, Atlas of Atomic Nuclear Structures according to Basic Structures of Matter theory, Journal of theoretics, 2003
www.journaloftheoretics.com/Links/Papers/Sarg2.pdf

7 S. Sarg, *Atlas of Atomic Nuclear Structures* (2001), National Library of Canada.
http://collection.nlc-bnc.ca/amicus/index-e.html (AMICUS No. 27106037)
also in http://www.helical-structures.org

8. I. Dabrowski, Can. J. Phys. **62**, 1639 (1984)

9. C. B. Anfinsen, J, T. Edsall and F. M. Richards, *Advances in protein chemistry*, vol. 34, 1981, Academic Press.

10. W. M. Gelbart, R. F. Bruinsma, P. A. Pincus and V. A. Parsegian, DNA-inspired electrostatics, Physics Today, 38-44, September (2000).

11. D. Bouwmeester et al, Observation of Three-Photon Greenberger-Horne_Zeilinger Entaglement, Phys. Rev. Lett., v. 82, No 7, 1345-1349, (1991)

12. A. Lamas-Linares, J. C. Howell & D. Bouwmeester, Stimulated emission of polarization-entangled photons, Nature, vol. 412, 887-890, (2001).

13. W. Saenger, *Principles of Nucleic Acid Structure*, Springer-Verlab, Ney York, (1984)

14.J. R. Lakowicz, B. Shen, Z. Gryczynski, S. D'Auria and I. Gryczynski, Intrinsic fluorescence from DNA can be enhanced by metalic particles, Biochemical and Biophysical Res. Comm., 286, 875-879 (2001)

15. Y. Kohwi and Y. Panchenko, Transcription-dependent recombination induced by triple-helix formation. Genes Dev. 7, 1766-1778, (1993)

16. C. Dekker, Electronic properties of DNA, Physics World, Aug. 2001
http://physicsweb.org/article/world/14/8/8

17. H-W Fink and C. Schonenberger, Electrical conduction through DNA molecule, Nature, **398**, 407, (1999)

18. D. Porath et al., Direct measurement of electrical transport through DNA molecules, Nature, **403**, 635, (2000)

19. S. Sarg, Theoretical analysis of biomolecules using BSM models (2002), archived in the National Library of Canada, http://collection.nlc-bnc.ca/amicus/index-e.html AMICUS No. 27749841